The Parkes multibeam pulsar survey – IV. Discovery of 180 pulsars and parameters for 281 previously known pulsars

G. Hobbs,[1]* A. Faulkner,[2] I. H. Stairs,[3] F. Camilo,[4] R. N. Manchester,[1] A. G. Lyne,[2] M. Kramer,[2] N. D'Amico,[5,6] V. M. Kaspi,[7] A. Possenti,[5] M. A. McLaughlin,[2] D. R. Lorimer,[2] M. Burgay,[5] B. C. Joshi[2,8] and F. Crawford[9]

[1]*Australia Telescope National Facility, CSIRO, PO Box 76, Epping NSW 1710, Australia*
[2]*University of Manchester, Jodrell Bank Observatory, Macclesfield, Cheshire SK11 9DL*
[3]*Department of Physics & Astronomy, University of British Columbia, 6224 Agricultural Road, Vancouver, B.C. V6T 1Z1, Canada*
[4]*Columbia Astrophysics Laboratory, Columbia University, 550 West 120th Street, New York, NY 10027, USA*
[5]*INAF - Osservatorio Astronomico di Cagliari, Loc. Poggio dei Pini, Strada 54, 09012, Capoterra (CA), Italy*
[6]*Universita' degli Studi di Cagliari, Dipartimento di Fisica, SP Monserrato-Sestu km 0,7, 90042, Monserrato (CA), Italy*
[7]*Physics Department, McGill University, Montreal, Quebec H3W 2C4, Canada*
[8]*National Centre for Radio Astrophysics, PO Bag No. 3, Ganeshkhind, Pune, India*
[9]*Department of Physics, Haverford College, Haverford, PA 19041, USA*

ABSTRACT

The Parkes multibeam pulsar survey has led to the discovery of more than 700 pulsars. In this paper, we provide timing solutions, flux densities and pulse profiles for 180 of these new discoveries. Two pulsars, PSRs J1736−2843 and J1847−0130, have rotational periods $P > 6$ s and are therefore among the slowest rotating radio pulsars known. Conversely, with $P = 1.8$ ms, PSR J1843−1113 has the third-shortest period of pulsars currently known. This pulsar and PSR J1905+0400 ($P = 3.8$ ms) are both solitary. We also provide orbital parameters for a new binary system, PSR J1420−5625, which has $P = 34$ ms, an orbital period of 40 d and a minimum companion mass of 0.4 solar masses. The 10°-wide strip along the Galactic plane that was surveyed is known to contain 264 radio pulsars that were discovered prior to the multibeam pulsar survey. We have redetected almost all of these pulsars and provide new dispersion measure values and flux densities at 20 cm for the redetected pulsars.

Key words: surveys – pulsars: general.

1 INTRODUCTION

Observing for the Parkes multibeam pulsar survey (hereafter referred to as the 'multibeam survey') has been completed. Full details of the telescope, hardware and software used were provided by Manchester et al. (2001) along with the rotational, astrometric and derived parameters for 100 pulsar discoveries. Morris et al. (2002) and Kramer et al. (2003) provided parameters for a further 320 discoveries timed for at least one year at the Parkes, Jodrell Bank and/or Arecibo observatories. Here, we provide timing solutions for 180 newly discovered pulsars. With this paper a total of 600 timing solutions for the multibeam discoveries have now been published.

We have successfully redetected 249 of the 264 previously known radio pulsars that lie within the survey region (defined by the Galactic coordinates $260° < l < 50°$ and $|b| < 5°$) and have redetected

a further 32 pulsars that lie outside this nominal survey region. For many of these redetected pulsars, the 35-min observation used during the survey is longer than any previous observation. Here, we analyse these long observations to obtain, for each pulsar, a flux density at 20 cm, pulse widths and dispersion measure. The flux densities are compared to other flux density measurements, at different observing frequencies, existing in the literature, to obtain new spectral indices for 38 pulsars.

This paper is divided into three major parts. In the first, we describe the observing systems used for the timing of the new multibeam survey discoveries and provide timing solutions for these pulsars. In the second, we highlight some particularly interesting discoveries such as the long-period pulsars PSRs J1736−2843 and J1847−0130, the solitary millisecond pulsars PSRs J1843−1113 and J1905+0400 and the binary system PSR J1420−5625. The third section contains a discussion on previously known pulsars redetected during the multibeam survey. We conclude by mentioning how these new results will be used to improve upon earlier studies of the Galactic pulsar population.

*E-mail: george.hobbs@csiro.au

© 2004 RAS

2 DISCOVERY AND TIMING OF 180 PULSARS

The pulsars detailed in this paper have been observed multiple (typically around 25) times for at least one year using the Parkes 64-m, the 305-m Arecibo and/or the 76-m Lovell telescopes. The observing and analysis methods used at Parkes and at Jodrell Bank were described by Manchester et al. (2001) and Morris et al. (2002) respectively. The Arecibo timing observations were taken with 100-MHz bandwidth centred at 1400 MHz, using the 'L-narrow' receiver with a system temperature of 25–30 K.[1] The incoming telescope voltages were sampled by the Wideband Arecibo Pulsar Processor (Dowd, Sisk & Hagen 2000), a digital correlator with three-level sampling, producing 128 lags across 100 MHz. Dual circular polarizations were summed in hardware, and 16-bit data samples written to disc every 64 μs. Typical integration times were 60 or 120 s. The data were then dedispersed and folded off-line modulo the predicted topocentric pulse period.

For every observation of each pulsar we obtained a pulse topocentric arrival time (TOA). Using the TEMPO program[2] we fitted a timing model, which contained the pulsar's position, rotational period and its derivative, to the TOAs of each pulsar. In Table 1 we provide these positions in equatorial and Galactic coordinates. Subsequent columns contain information on the discovery of each pulsar: the beam number (corresponding to the 13 beams of the multibeam receiver) for the highest signal-to-noise ratio (S/N) discovery observation of this pulsar, the radial distance between the centre of this beam and the position of the pulsar (beam radii greater than one beamwidth occur if the pulsar scintillates or nulls or the closest pointing was contaminated by interference) and the S/N of the profile during this observation. The observations used to form TOAs were added together to provide a characteristic pulse profile for each pulsar at 1374 MHz (Fig. 1). The final three columns in Table 1 contain the flux densities measured from these mean profiles and the pulse widths at 50 and 10 per cent of the pulse height. The 10 per cent width is not measurable for pulsars with mean profiles that have poor signal-to-noise ratios. For profiles containing multiple components the widths are measured across the entire profile.

Some of the profiles observed at Arecibo had significant dips at the start of the observed pulse shape. These are due to instrumental data quantization problems. For cases where dips remained even after applying a correction scheme (Van Vleck & Middleton 1966), we used Parkes observations to determine the flux density and pulse widths (and provide the profile obtained at Parkes in Fig. 1) if high S/N profiles were available. For the remaining pulsars that were observed at the Arecibo Observatory, flux densities were obtained using estimates of the gain and system temperatures (these vary significantly with zenith angle and were therefore found separately for each observation[3]). The sky temperature at each position was estimated from Haslam et al. (1982) assuming a spectral index of −2.5 (Reich & Reich 1988). The scale was determined by comparing the baseline noise with the predictions of the radiometer equation and flux densities were found by integrating under the peak of each profile. Individual observations were averaged to find the mean flux density for each pulsar. This was then corrected for off-centre pointing by assuming a Gaussian beam-shape with a beamwidth of

3.6 arcmin. Estimated uncertainties for all parameters are given in parentheses where relevant and refer to the last quoted digit.

The rotational parameters of the pulsars are given in Table 2. In column order, this table provides the name of each pulsar, solar-system barycentric pulse period, period derivative, epoch of the period, the number of TOAs used in the timing solution, the MJD range covered by the timing observations, the final root-mean-square values for the timing residuals and the dispersion measure. The data have been folded at two and three times the tabulated periods in order to confirm that they represent the fundamental periods of the pulsars. Pulsars timed primarily at Arecibo or Jodrell Bank are indicated by a superscript '*A*' or '*J*' respectively; all other pulsars were timed using the Parkes telescope. PSRs J1016−5857 and J1437−6146 have both glitched. Table 2 contains their post-glitch solution; full details of the glitches will be provided in a later paper. A pre-glitch timing solution for PSR J1016−5857 has also been published by Camilo et al. (2001a). A timing solution for PSR J1847−0130 was previously published by McLaughlin et al. (2003a).

Five pulsars in our sample were independently discovered by other surveys. We define pulsars as independent discoveries if our confirmation of the pulsar candidate occurred prior to the parameters of the pulsar being published elsewhere. Three, PSRs J0843−5022, J1352−6803 and J1415−6621, were detected in the Swinburne multibeam pulsar survey (Edwards et al. 2001). The timing solution given in Tables 1 and 2 for PSR J0843−5022 was obtained from Edwards et al. (2001). Bailes (2003; private communication) provided a timing solution for PSR J1415−6621 and the solution for PSR J1352−6803 was obtained from our observations. PSR J1907+0918 was discovered by Lorimer & Xilouris (2000) during a search for radio emission from SGR 1900+14. The timing solution given in Tables 1 and 2 is obtained from Lorimer & Xilouris (2000). The flux density and pulse widths were obtained from the Parkes multibeam data. The flux density tabulated of 0.29(4) mJy agrees well with the earlier measurement of 0.3(1) mJy. PSR J1435−5954 was independently discovered at Parkes in an unpublished pulsar search during the year 1995. We provide a timing solution from observations between 1995 and 1998.

PSR J1420−5625 is a 34-ms pulsar in a 40-d binary system. The orbital parameters for this intermediate-mass binary pulsar system are given in Table 3 and discussed in Section 3.1.2. All published parameters may also be obtained online using the ATNF pulsar catalogue[4] (Manchester et al., in preparation).

3 DISCUSSION

This discussion section is in two parts: we first describe the newly discovered pulsars and second discuss those that were detected, but not discovered, during the multibeam survey.

3.1 New discoveries

In Table 4 we list the derived parameters of the pulsars: the logarithm of the characteristic age in years, the surface dipole magnetic field strength, $B_s = 3.2 \times 10^{19} (P\dot{P})^{1/2}$ in gauss, and the rate of loss of rotational energy in erg s^{-1} where a neutron star with moment of inertia 10^{45} g cm^2 is assumed. The final columns contain the pulsar distances and luminosities. The distances are computed from their dispersion measures assuming the Taylor & Cordes (1993) model for the Galactic distribution of free electrons. This model is

---

[1] See http://www.naic.edu/~astro/RXstatus for further technical details of this receiver

[2] See http://www.atnf.csiro.au/research/pulsar/tempo/

[3] See http://www.naic.edu/~astro/RXstatus/Lnarrow/ln_gain_postaug01.shtml and http://www.naic.edu/~astro/RXstatus/Lnarrow/ln_tsys_2001.shtml

[4] http://www.atnf.csiro.au/research/pulsar/psrcat

Table 1. Positions, flux densities and pulse widths for 180 pulsars discovered in the Parkes multibeam pulsar survey. Radial angular distances are given in units of beam radii. Timing solutions indicated by a *J* or an *A* have a significant number of observations from the Jodrell Bank and Arecibo telescopes, respectively. Pulse widths at 10 per cent of the peak are given only for high signal-to-noise ratio profiles.

PSR J	R.A. (J2000) (h m s)	Dec. (J2000) (° ′ ″)	l (°)	b (°)	Beam	Radial distance	S/N	S_{1400} (mJy)	W_{50} (ms)	W_{10} (ms)
0843−5022	08:43:09.884(8)	−50:22:43.10(8)	268.50	−4.90	7	0.46	31.6	0.31(4)	6.1	29
1016−5857	10:16:21.16(1)	−58:57:12.1(1)	284.08	−1.88	3	0.74	22.3	0.46(5)	7.8	–
1021−5601	10:21:24.82(15)	−56:01:50.9(11)	283.04	0.94	7	0.77	21.8	0.37(5)	52.0	–
1032−5206	10:32:27.69(7)	−52:06:08.5(6)	282.35	5.13	11	0.64	34.7	0.19(3)	21.0	71
1052−6348	10:52:53.39(6)	−63:48:16.6(3)	290.29	−3.88	3	0.49	9.5	0.11(2)	10.0	–
1054−6452	10:54:08.84(16)	−64:52:37.5(8)	290.89	−4.78	8	1.00	22.2	0.25(4)	22.0	42
1055−6022	10:55:48.5(4)	−60:22:52(3)	289.11	−0.65	13	0.90	10.9	0.16(3)	23.0	–
1106−6438	11:06:28.44(14)	−64:38:60.0(6)	291.99	−4.03	10	0.63	23.4	0.19(3)	27.0	46
1152−5800	11:52:10.0(4)	−58:00:34(4)	295.13	3.96	5	0.71	10.2	0.12(2)	16.0	–
1156−5707	11:56:07.45(4)	−57:07:01.9(5)	295.45	4.95	7	0.76	14.1	0.19(3)	4.8	17
1210−6550	12:10:42.0(3)	−65:50:04.6(19)	298.77	−3.29	11	0.91	15.5	0.17(3)	39.0	–
1337−6306	13:37:20.35(5)	−63:06:23.3(3)	308.10	−0.70	1	0.82	8.7	0.11(2)	12.0	–
1352−6803	13:52:34.44(3)	−68:03:36.79(19)	308.61	−5.87	12	1.77	17.4	0.68(8)	28.0	45
1415−6621	14:15:31.27(3)	−66:21:12.2(3)	311.23	−4.85	6	0.18	97.8	0.71(8)	8.9	17
1420−5625	14:20:03.062(3)	−56:25:55.00(3)	315.00	4.35	8	0.86	12.3	0.13(2)	1.3	12
1424−5556	14:24:12.76(3)	−55:56:13.9(3)	315.72	4.61	6	0.65	40.3	0.38(5)	22.0	36
1435−5954	14:35:00.36(5)	−59:54:49.2(3)	315.58	0.39	1	0.75	96.1	3.6(4)	19.0	33
1437−6146	14:37:15.31(9)	−61:46:02.0(8)	315.10	−1.42	13	0.43	19.4	0.24(3)	17.0	–
1502−5653	15:02:57.389(11)	−56:53:39.21(12)	320.19	1.51	3	0.74	46.3	0.39(5)	7.2	14
1519−6308	15:19:09.56(18)	−63:08:19.5(10)	318.74	−4.90	1	0.55	45.0	0.32(4)	22.0	–
1538−5551	15:38:45.03(4)	−55:51:36.9(6)	324.91	−0.30	1	0.87	10.6	0.25(4)	11.0	–
1542−5133	15:42:19.93(13)	−51:33:35(3)	327.91	2.83	7	0.97	19.7	0.27(4)	35.0	59
1547−5750	15:47:30.60(10)	−57:50:29.4(15)	324.66	−2.60	11	0.20	27.3	0.23(3)	39.0	–
1551−5310	15:51:41.25(6)	−53:10:59.6(8)	328.03	0.67	5	0.97	18.2	0.54(6)	62.0	–
1609−4616	16:09:41.13(4)	−46:16:22.5(4)	334.76	3.99	12	0.28	36.6	0.38(5)	5.6	9
1620−5414	16:20:14.44(10)	−54:14:51.7(16)	330.47	−2.94	4	0.82	11.4	0.13(2)	26.0	–
1632−4509	16:32:14.00(17)	−45:09:09(9)	338.34	2.00	11	0.06	14.4	0.16(3)	18.0	–
1632−4757	16:32:16.72(6)	−47:57:34.3(14)	336.30	0.08	8	0.97	9.5	0.30(4)	21.0	–
1638−4417	16:38:46.221(14)	−44:17:03.6(4)	339.77	1.73	12	0.88	12.2	0.21(3)	5.6	–
1658−4958	16:58:54.92(6)	−49:58:58.4(6)	337.60	−4.55	9	0.94	64.7	0.87(10)	13.0	26
1700−3919	17:00:22.27(3)	−39:19:00.02(142)	346.16	1.83	11	0.26	23.2	0.23(3)	14.0	–
1702−4217	17:02:36.44(6)	−42:17:01.2(22)	344.08	−0.33	13	0.48	18.4	0.50(6)	41.0	–
1708−4522	17:08:12.92(6)	−45:22:51(3)	342.22	−3.01	1	0.63	25.1	0.22(3)	17.0	37
1715−4254	17:15:10.54(9)	−42:54:54(4)	344.95	−2.56	6	0.71	9.5	0.07(2)	26.0	–
1718−3714	17:18:18.59(16)	−37:14:16(9)	349.93	0.24	11	0.42	9.5	0.23(3)	96.0	–
1718−3718	17:18:10.0(3)	−37:18:53(11)	349.85	0.22	11	0.27	13.3	0.18(3)	130.0	–
1724−3149	17:24:44.87(7)	−31:49:04(4)	355.14	2.23	11	0.42	24.9	0.36(5)	32.0	–
1726−4006	17:26:33.37(7)	−40:06:02(4)	348.48	−2.71	4	0.86	17.7	0.21(3)	20.0	–
1727−2739	17:27:30.99(12)	−27:39:00.5(169)	358.94	4.05	11	0.80	79.5	1.60(17)	90.0	–
1730−3353	17:30:55.58(10)	−33:53:38(12)	354.14	−0.00	3	0.38	43.9	0.38(5)	54.0	–
1731−3123	17:31:00.53(3)	−31:23:43(4)	356.23	1.35	6	1.06	14.7	0.29(4)	19.0	–
1732−4156	17:32:48.86(4)	−41:56:29.6(16)	347.59	−4.71	5	0.67	17.9	0.22(3)	21.0	–
1733−3030	17:33:58.89(6)	−30:30:49(7)	357.32	1.30	13	0.64	10.2	0.20(3)	16.0	–
1733−4005	17:33:58.64(3)	−40:05:39.7(15)	349.27	−3.89	13	0.71	40.0	0.49(6)	14.0	23
1736−2819	17:36:24.73(9)	−28:19:42(16)	359.45	2.04	7	0.78	10.3	0.16(3)	21.0	–
1736−2843	17:36:42.59(16)	−28:43:51(22)	359.14	1.76	1	0.63	47.4	0.43(5)	145.0	–
1737−3320	17:37:10.51(5)	−33:20:20(5)	355.31	−0.79	5	0.40	22.2	0.35(4)	42.0	–
1738−2647	17:38:05.03(4)	−26:47:46(26)	0.94	2.54	12	0.93	20.6	0.44(5)	12.0	–
1738−3107	17:38:47.4(3)	−31:07:44(14)	357.36	0.10	12	1.04	12.0	0.26(4)	34.0	–
1738−3316	17:38:34.45(6)	−33:16:01.6(49)	355.53	−1.00	9	0.70	21.0	0.55(7)	91.0	–

Table 1 – *continued*

PSR J	R.A. (J2000) (h m s)	Dec. (J2000) (° ′ ″)	l (°)	b (°)	Beam	Radial distance	S/N	S_{1400} (mJy)	W_{50} (ms)	W_{10} (ms)
1740−2540	17:40:45.32(6)	−25:40:19(18)	2.21	2.63	6	0.21	17.6	0.16(3)	30.0	–
1740−3327	17:40:25.72(3)	−33:27:53.5(17)	355.56	−1.44	3	1.08	15.8	0.30(4)	11.0	23
1743−2442	17:43:20.12(10)	−24:42:55(41)	3.33	2.64	4	0.38	14.8	0.14(2)	75.0	–
1745−2229	17:45:16.71(7)	−22:29:14(25)	5.47	3.42	12	0.33	18.9	0.13(2)	14.0	–
1749−2347	17:49:15.61(12)	−23:47:17(82)	4.83	1.97	5	1.40	11.5	0.13(2)	9.1	–
1750−2444	17:50:22.96(8)	−24:44:47(42)	4.14	1.26	13	0.50	15.7	0.27(4)	32.0	–
1752−2410	17:52:58.742(15)	−24:10:26(15)	4.93	1.04	10	2.71	30.2	0.47(6)	7.1	–
1754−3443	17:54:37.372(14)	−34:43:53.9(10)	355.99	−4.61	8	0.91	33.4	0.49(6)	12.0	21
1755−25211	17:55:19.31(5)	−25:21:09(18)	4.18	−0.02	6	0.26	15.1	0.17(3)	20.0	–
1755−2534	17:55:49.82(3)	−25:34:39(11)	4.05	−0.23	10	0.29	9.2	0.17(3)	15.0	–
1756−2225	17:56:25.56(8)	−22:25:48(66)	6.84	1.24	1	0.67	17.0	0.25(4)	19.0	–
1758−1931	17:58:05.60(7)	−19:31:41(11)	9.54	2.35	6	0.79	20.4	0.38(5)	21.0	–
1759−1903	17:59:41.76(16)	−19:03:19(27)	10.14	2.26	2	0.39	16.4	0.16(3)	34.0	–
1759−3107	17:59:22.056(14)	−31:07:21.5(20)	359.63	−3.67	10	0.99	97.8	0.91(10)	16.0	27
1800−2114	18:00:12.3(4)	−21:14:19(75)	8.31	1.07	1	0.56	18.7	0.30(4)	90.0	–
1801−2115	18:01:32.49(12)	−21:15:18(53)	8.45	0.79	1	0.46	12.0	0.19(3)	47.0	–
1801−2154	18:01:08.33(3)	−21:54:32(12)	7.83	0.55	11	0.49	15.0	0.18(3)	9.6	–
1803−1616	18:03:34.68(3)	−16:16:30(4)	13.02	2.83	5	0.55	16.9	0.16(3)	19.0	–
1803−1920	18:03:29.44(3)	−19:20:41(7)	10.33	1.34	9	0.49	18.6	0.27(4)	12.0	–
1805−2447	18:05:25.93(3)	−24:47:30(14)	5.81	−1.72	3	0.88	13.6	0.27(4)	11.0	22
1806−1618	18:06:25.78(6)	−16:18:38(8)	13.32	2.21	11	0.53	11.9	0.22(3)	34.0	–
1809−1850	18:09:37.21(12)	−18:50:55(21)	11.47	0.32	6	0.93	13.0	0.20(3)	55.0	–
1810−1441	18:10:59.162(14)	−14:41:33.6(13)	15.27	2.03	5	0.96	10.6	0.21(3)	14.0	–
1812−1910	18:12:34.89(10)	−19:10:39(10)	11.52	−0.46	4	0.88	10.2	0.22(3)	28.0	–
1813−2242	18:13:29.16(8)	−22:42:06(42)	8.53	−2.33	8	0.75	11.9	0.21(3)	21.0	–
1815−1738	18:15:14.672(9)	−17:38:03.0(12)	13.18	−0.27	1	0.58	13.9	0.25(4)	29.0	–
1816−1446	18:16:29.19(3)	−14:46:30(3)	15.84	0.83	3	0.16	17.5	0.23(3)	25.0	–
1817−1511^J	18:17:36.20(6)	−15:11:39(6)	15.59	0.39	2	0.24	18.9	0.43(5)	21.0	–
1818−1116^J	18:18:26.45(6)	−11:16:29(7)	19.14	2.07	11	0.11	23.2	0.50(6)	25.0	–
1819−0925^J	18:19:50.542(19)	−09:25:49.9(13)	20.93	2.63	9	0.68	60.0	0.72(8)	20.0	34
1819−1008^J	18:19:39.986(17)	−10:08:28(4)	20.29	2.34	1	0.73	21.4	0.35(4)	9.9	–
1819−1131	18:19:58.15(10)	−11:31:29(9)	19.10	1.62	7	0.37	10.8	0.15(3)	64.0	–
1820−1529^J	18:20:40.82(9)	−15:29:50(10)	15.68	−0.41	11	0.24	19.6	0.61(7)	28.0	–
1821−1419	18:21:34.3(4)	−14:19:26(32)	16.82	−0.04	12	0.20	11.1	0.20(3)	99.0	–
1822−0907	18:22:39.80(5)	−09:07:36(3)	21.53	2.16	1	0.71	11.4	0.12(2)	28.0	–
1822−1252	18:22:41.7(3)	−12:52:49(29)	18.22	0.39	7	0.27	15.0	0.25(4)	105.0	–
1822−1617	18:22:36.6(3)	−16:17:35(25)	15.19	−1.19	6	0.34	9.8	0.20(3)	115.0	–
1823−1126	18:23:19.86(10)	−11:26:04(5)	19.57	0.93	9	0.68	36.4	0.51(6)	23.0	44
1823−1526	18:23:21.42(6)	−15:26:22(7)	16.03	−0.95	5	0.75	26.8	0.47(6)	41.0	–
1824−1500	18:24:14.10(7)	−15:00:33(8)	16.51	−0.93	1	0.86	10.9	0.16(3)	18.0	–
1828−0611	18:28:20.715(6)	−06:11:51.5(4)	24.78	2.28	10	0.60	68.3	1.20(13)	10.0	19
1828−1007	18:28:30.356(15)	−10:07:10.1(10)	21.32	0.42	12	0.53	11.2	0.21(3)	8.7	–
1828−1057	18:28:33.21(4)	−10:57:26(3)	20.59	0.02	13	0.67	11.7	0.23(3)	15.0	–
1831−0823^J	18:31:36.334(8)	−08:23:23.9(5)	23.21	0.55	12	0.66	78.8	0.97(11)	14.0	23
1831−1423	18:31:29.10(3)	−14:23:46(4)	17.87	−2.20	11	0.11	13.3	0.19(3)	23.0	–
1833−0556	18:33:38.88(16)	−05:56:05(9)	25.62	1.23	7	0.57	11.4	0.20(3)	69.0	–
1834−0633	18:34:29.25(15)	−06:33:01.1(63)	25.17	0.76	6	0.43	17.8	0.28(4)	101.6	–
1834−0731	18:34:16.00(7)	−07:31:07(4)	24.29	0.37	4	0.44	46.3	1.00(11)	30.0	–
1834−0742^J	18:34:31.32(3)	−07:42:20.6(14)	24.15	0.22	2	0.22	27.4	0.35(4)	18.0	–
1834−1202	18:34:23.12(3)	−12:02:26.4(13)	20.29	−1.74	2	1.01	26.4	0.70(8)	63.0	87

Table 1 – *continued*

PSR J	R.A. (J2000) (h m s)	Dec. (J2000) (° ′ ″)	l (°)	b (°)	Beam	Radial distance	S/N	S_{1400} (mJy)	W_{50} (ms)	W_{10} (ms)
1835−0522	18:35:08.12(5)	−05:22:08(3)	26.30	1.16	6	0.76	18.4	0.23(3)	23.0	–
1836−0517	18:36:25.20(11)	−05:17:35(4)	26.51	0.91	1	0.89	9.5	0.15(3)	13.0	–
1838−0549	18:38:38.09(3)	−05:49:12(3)	26.30	0.18	11	0.37	18.9	0.29(4)	7.0	–
1838−0624	18:38:51.78(11)	−06:24:54(4)	25.79	−0.14	5	0.54	10.9	0.16(3)	36.0	–
1839−0905	18:39:53.458(20)	−09:05:14.8(14)	23.53	−1.59	13	0.69	12.1	0.16(3)	17.0	–
1840−0559	18:40:23.18(4)	−05:59:16.2(18)	26.35	−0.28	12	1.16	12.7	0.31(4)	16.0	34
1840−0809[J]	18:40:33.364(6)	−08:09:03.3(4)	24.44	−1.31	1	1.02	134.2	2.3(2)	10.0	35
1840−0815[J]	18:40:13.775(13)	−08:15:10.6(7)	24.31	−1.28	1	1.79	19.6	1.40(15)	22.0	35
1840−1122	18:40:24.066(19)	−11:22:10.7(16)	21.56	−2.74	3	0.87	14.5	0.13(2)	11.0	–
1841−0157[J]	18:41:56.207(20)	−01:57:54.6(8)	30.10	1.22	9	0.35	97.7	0.81(9)	21.0	–
1841−0310	18:41:25.89(14)	−03:10:21(9)	28.97	0.78	13	0.39	14.1	0.15(3)	59.0	–
1841−0524	18:41:49.32(5)	−05:24:29.5(12)	27.02	−0.33	3	0.59	13.1	0.20(3)	13.0	–
1842−0309	18:42:19.02(5)	−03:09:46(3)	29.08	0.58	9	0.64	11.5	0.25(4)	43.0	–
1842−0612	18:42:43.05(10)	−06:12:36(5)	26.41	−0.90	12	0.61	21.7	0.54(6)	53.0	–
1843−0000[J]	18:43:27.962(9)	−00:00:40.9(6)	32.01	1.77	10	0.62	250.4	2.9(3)	26.0	40
1843−0137	18:43:12.63(3)	−01:37:46.3(12)	30.54	1.09	4	1.04	13.5	0.26(4)	17.0	–
1843−0211	18:43:30.328(20)	−02:11:02.8(7)	30.08	0.77	10	0.65	69.8	0.93(10)	24.0	105
1843−0408	18:43:43.44(7)	−04:08:04(3)	28.37	−0.17	9	0.60	17.1	0.17(3)	12.0	–
1843−0702	18:43:22.441(10)	−07:02:54.6(7)	25.74	−1.43	3	0.40	20.1	0.17(3)	4.7	–
1843−0806	18:43:28.715(11)	−08:06:44.9(7)	24.81	−1.93	12	0.97	13.5	0.36(5)	21.0	–
1843−1113	18:43:41.26225(20)	−11:13:31.052(16)	22.05	−3.40	7	0.18	17.6	0.10(2)	0.2	–
1844−0030[A]	18:44:41.099(19)	−00:30:25.8(13)	31.71	1.27	5	0.61	33.5	0.42(5)	16.0	–
1844−0452	18:44:01.54(4)	−04:52:20.9(19)	27.75	−0.58	9	0.84	8.7	0.19(3)	16.0	–
1844−0502	18:44:33.96(7)	−05:02:00.5(23)	27.67	−0.77	5	1.06	10.2	0.40(5)	24.0	–
1845−0545	18:45:38.49(4)	−05:45:18.2(10)	27.15	−1.34	10	0.97	20.9	0.47(6)	18.0	32
1846+0051[A]	18:46:43.821(20)	+00:51:39.0(7)	33.16	1.44	11	1.02	16.9	0.34(9)	28.2	60
1847−0130	18:47:35.21(9)	−01:30:46(3)	31.15	0.17	3	0.41	15.6	0.33(4)	205.0	–
1847−0443	18:47:51.85(3)	−04:43:36.2(8)	28.32	−1.36	7	0.62	11.1	0.16(3)	9.0	–
1848−0023[A]	18:48:37.89(9)	−00:23:17(4)	32.27	0.45	7	1.23	13.1	0.6(3)	17.7	38
1848−0055	18:48:45.50(19)	−00:55:53(4)	31.80	0.17	6	0.65	9.5	0.19(3)	27.9	–
1848−0511	18:48:15.01(14)	−05:11:38(5)	27.95	−1.66	8	0.25	21.4	0.40(5)	99.0	–
1849−0040[A]	18:49:10.25(8)	−00:40:20(6)	32.08	0.20	11	0.34	10.9	0.20(3)	64.6	–
1849−0614	18:49:45.157(19)	−06:14:31.5(8)	27.18	−2.47	3	1.18	36.8	0.59(7)	14.0	32
1850−0031	18:50:33.39(9)	−00:31:09(4)	32.37	−0.04	11	0.93	9.3	0.23(3)	32.0	–
1851+0118	18:51:52.18(13)	+01:18:59(5)	34.15	0.50	1	0.95	10.9	0.10(2)	24.0	–
1851−0053[A]	18:51:03.17(8)	−00:53:07.3(19)	32.10	−0.32	5	1.24	35.9	1.00(11)	19.0	–
1851−0241	18:51:15.26(10)	−02:41:31(3)	30.51	−1.19	4	0.56	10.9	0.20(3)	35.0	–
1852+0008[A]	18:52:42.78(3)	+00:08:09.6(8)	33.20	−0.22	5	0.58	15.8	0.31(4)	16.0	–
1852+0013[A]	18:52:41.779(20)	+00:13:57.1(12)	33.28	−0.17	5	0.22	14.8	0.30(4)	19.0	–
1852−0118	18:52:17.15(3)	−01:18:14.8(17)	31.87	−0.78	6	0.98	22.1	0.35(4)	24.0	–
1852−0127	18:52:03.60(4)	−01:27:23.4(14)	31.71	−0.80	6	0.34	36.1	0.58(7)	18.0	–
1852−0635	18:52:57.38(14)	−06:35:57(8)	27.22	−3.34	12	0.86	160.4	5.9(6)	90.0	–
1853+0011[A]	18:53:29.968(14)	+00:11:29.7(5)	33.34	−0.37	6	0.34	8.3	0.30(8)	11.8	21
1853+0505	18:53:04.36(7)	+05:05:26.1(18)	37.65	1.96	9	1.03	67.4	1.50(16)	92.0	195
1853−0004[A]	18:53:23.018(6)	−00:04:32.3(4)	33.09	−0.47	3	0.76	22.5	0.87(10)	2.2	6
1855+0307[A]	18:55:26.63(3)	+03:07:20.2(9)	36.17	0.53	4	0.94	31.1	0.97(11)	12.0	–
1855+0700	18:55:17.72(4)	+07:00:37.1(9)	39.61	2.34	4	0.95	11.0	0.10(2)	5.4	–
1856+0102[A]	18:56:28.503(13)	+01:02:10.6(5)	34.43	−0.65	3	0.54	11.4	0.38(11)	16.8	28
1857+0143[A]	18:57:33.008(15)	+01:43:47.0(9)	35.17	−0.57	4	0.41	29.9	0.74(18)	15.7	43
1857+0809	18:57:09.31(3)	+08:09:04.3(8)	40.84	2.45	12	0.23	14.4	0.14(2)	12.0	–

Table 1 – *continued*

PSR J	R.A. (J2000) (h m s)	Dec. (J2000) (° ′ ″)	l (°)	b (°)	Beam	Radial distance	S/N	S_{1400} (mJy)	W_{50} (ms)	W_{10} (ms)
1858+0241	18:58:53.81(14)	+02:41:38(6)	36.18	−0.43	6	0.09	11.9	0.10(2)	80.0	–
1859+0601[A]	18:59:45.76(5)	+06:01:46.1(18)	39.25	0.90	6	0.83	12.1	0.30(4)	24.3	–
1900+0634[A]	19:00:28.034(20)	+06:34:20.9(6)	39.81	1.00	12	0.54	11.7	0.24(9)	11.1	20
1900−0051[J]	19:00:46.644(7)	−00:51:08.4(5)	33.24	−2.47	5	1.00	30.1	0.45(6)	5.6	17
1901+0124[A]	19:01:52.545(14)	+01:24:49.3(8)	35.38	−1.68	12	1.06	13.2	0.30(4)	8.3	–
1901+0254	19:01:15.67(7)	+02:54:41(5)	36.64	−0.86	11	0.74	42.8	0.58(7)	70.0	–
1901+0320[A]	19:01:03.01(9)	+03:20:18(4)	37.00	−0.61	8	0.42	10.4	0.89(10)	47.2	–
1901+0355	19:01:30.81(4)	+03:55:58.9(9)	37.58	−0.44	1	0.33	15.9	0.15(3)	12.0	–
1901+0510[A]	19:01:57.85(11)	+05:10:34(4)	38.74	0.03	10	1.51	8.6	0.66(8)	56.9	–
1901−0312	19:01:15.675(18)	−03:12:29.5(9)	31.19	−3.65	7	0.74	16.3	0.23(3)	7.9	–
1902+0248	19:02:50.26(7)	+02:48:56(3)	36.74	−1.25	5	1.24	11.7	0.17(3)	35.4	–
1902−0340	19:02:50.70(19)	−03:40:18(4)	30.96	−4.21	6	0.48	16.5	0.22(3)	25.0	–
1903+0601[J]	19:03:20.874(16)	+06:01:34.0(6)	39.65	0.11	11	1.03	12.7	0.26(4)	12.0	–
1905+0400	19:05:28.2736(3)	+04:00:10.922(13)	38.09	−1.29	4	1.10	26.5	0.050(10)	0.6	–
1905+0600	19:05:04.35(5)	+06:00:59.9(14)	39.84	−0.28	8	0.83	17.4	0.42(5)	13.0	–
1906+0649[A]	19:06:11.97(3)	+06:49:48.1(10)	40.69	−0.15	11	0.25	36.4	0.30(4)	37.0	–
1907+0249[A]	19:07:42.03(4)	+02:49:41(3)	37.31	−2.32	11	1.03	10.7	0.46(12)	21.7	32
1907+0345	19:07:14.543(19)	+03:45:10.6(4)	38.08	−1.80	1	0.62	13.3	0.17(3)	6.3	–
1907+0731	19:07:54.79(3)	+07:31:21.9(5)	41.50	−0.21	7	1.21	20.9	0.35(4)	11.0	–
1907+0918	19:07:22.441(4)	+09:18:30.76(4)	43.02	0.73	3	0.97	12.8	0.29(4)	4.4	–
1910+0225[A]	19:10:10.359(17)	+02:25:23.6(5)	37.23	−3.06	7	0.25	39.2	0.6(2)	16.4	29
1910+0728	19:10:22.079(6)	+07:28:37.09(15)	41.74	−0.77	11	0.52	78.2	0.87(10)	15.0	22
1913+1000	19:13:03.59(5)	+10:00:02.4(14)	44.29	−0.19	2	0.48	42.5	0.53(6)	32.0	52
1914+0631[A]	19:14:17.24(4)	+06:31:56.3(10)	41.35	−2.07	11	0.83	15.6	0.26(10)	12.6	27
1915+0838[J]	19:15:13.87(3)	+08:38:59.7(13)	43.34	−1.30	13	1.17	13.5	0.29(4)	14.0	–
1916+0844[J]	19:16:19.081(9)	+08:44:07.0(4)	43.54	−1.49	10	1.03	30.1	0.44(5)	8.3	19
1916+0852	19:16:24.6(3)	+08:52:36(5)	43.67	−1.45	4	0.75	16.4	0.13(2)	48.0	–
1916+1023[A]	19:16:36.91(15)	+10:23:03(6)	45.03	−0.79	4	0.20	29.7	0.36(5)	72.0	–
1920+1040[A]	19:20:55.38(8)	+10:40:31(3)	45.78	−1.59	11	0.39	47.8	0.57(7)	45.0	–
1937+1505[J]	19:37:16.31(14)	+15:05:19(4)	51.57	−2.98	8	0.76	11.3	0.13(2)	46.0	–

used, rather than the more recent Cordes & Lazio (2002) or Gómez, Benjamin & Cox (2002) models, for consistency with the distance and luminosity values provided in earlier papers of this series. The implications of using the Cordes & Lazio (2002) model for the determination of the distances and luminosities of the multibeam pulsars was described by Kramer et al. (2003). In general, the distances are less accurate than the 0.1 kpc quoted because of uncertainties in the electron density model.

3.1.1 Rotational properties

A P–$\dot{P}$ diagram is shown in Fig. 2 with the 180 new discoveries presented in this paper highlighted (open circles). Three of these pulsars (PSRs J1821−1419, J1718−3718 and J1847−0130) lie just inside a region of the diagram that is expected to be radio quiet (Baring & Harding 2001). However, the exact position of the boundary that defines this region is not well determined and, for instance, depends upon the poorly known height of the radio emission above the surface of the neutron star. Two of these pulsars, PSRs J1718−3718 and J1847−0130, have rotational parameters similar to the anomalous X-ray pulsars (diamond symbols in Fig. 2) and have already been discussed by McLaughlin et al. (2003a,b). PSRs J1847−0130

and J1736−2843 have rotational periods greater than six seconds and are the second and third-slowest rotating radio pulsars known. However, even with its long rotational period, PSR J1736−2843 lies in the P–$\dot{P}$ diagram below the 'radio-quiet' boundary and above the death-line.

Our sample also includes the solitary millisecond pulsars, PSRs J1843−1113 ($P = 1.85$ ms) and J1905+0400 ($P = 3.78$ ms). PSR J1843−1113 is the third-fastest rotating pulsar known (after PSRs B1937+21 and B1957+20 which have spin periods of 1.56 and 1.61 ms respectively). We reported in earlier multibeam papers that the multibeam survey had discovered fewer recycled pulsars than expected (see also Toscano et al. 1998). This lack of recycled pulsars was partly due to a poor choice of software filters that were applied to remove known interference before searching begins for pulsar candidates. Hobbs (2002) showed that significant increases in the detection rates of millisecond pulsars could be made by improving these filters. The multibeam data are currently being reanalysed with updated search code. A full description of this reprocessing will be published by Faulkner et al. (in preparation).

Bailes et al. (1997) reported on the discovery of four isolated millisecond pulsars. Three of these have very low luminosities while the other had a more intermediate luminosity. They concluded that the
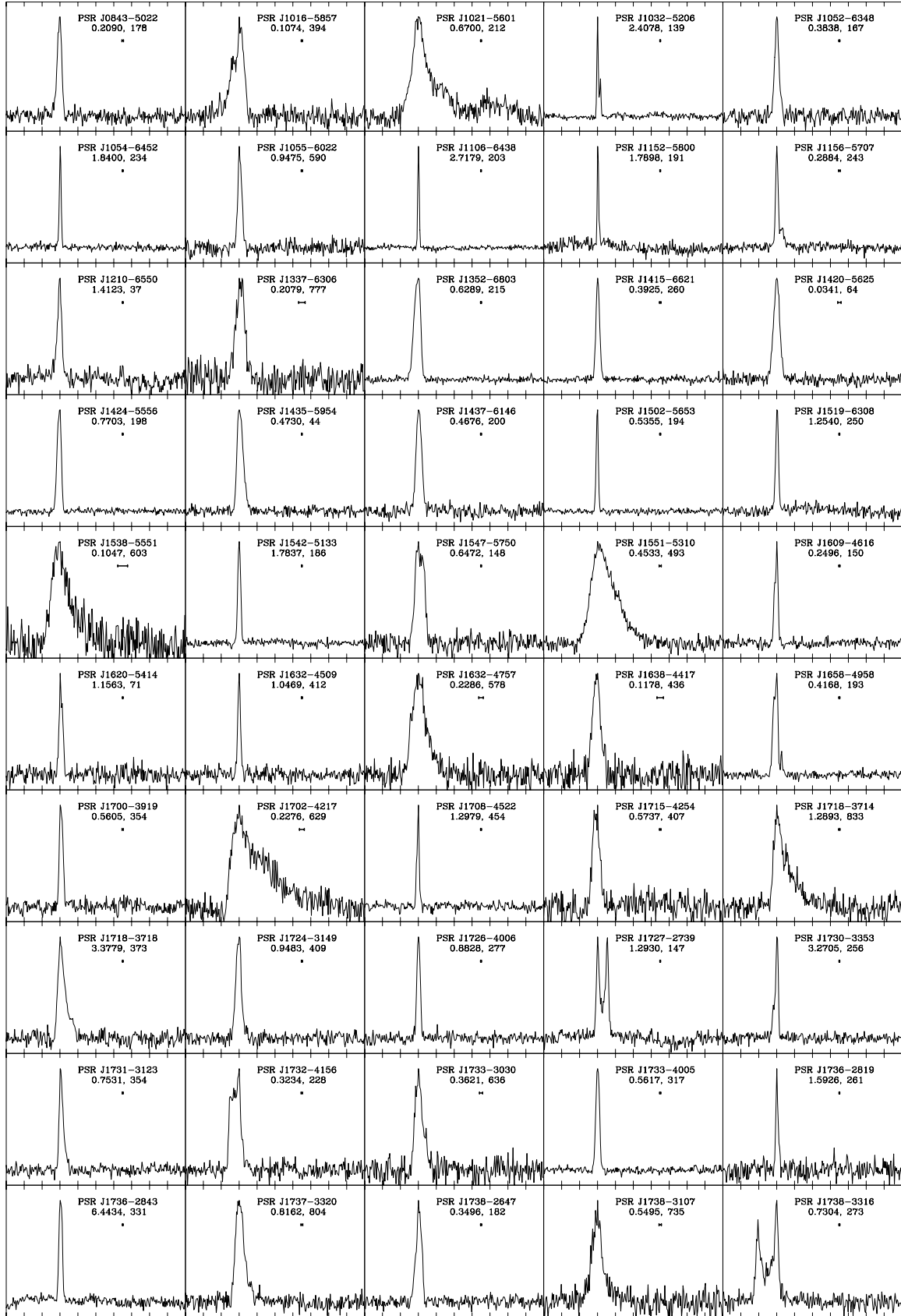
Figure 1. Mean 1374-MHz pulse profiles for 180 pulsars discovered in the multibeam survey. The highest point in the profile is placed at phase 0.3. For each profile, the pulsar Jname, pulse period (s) and dispersion measure (cm^{-3} pc) are given. The small horizontal bar under the period indicates the effective resolution of the profile by adding the bin size to the effects of interstellar dispersion in quadrature.
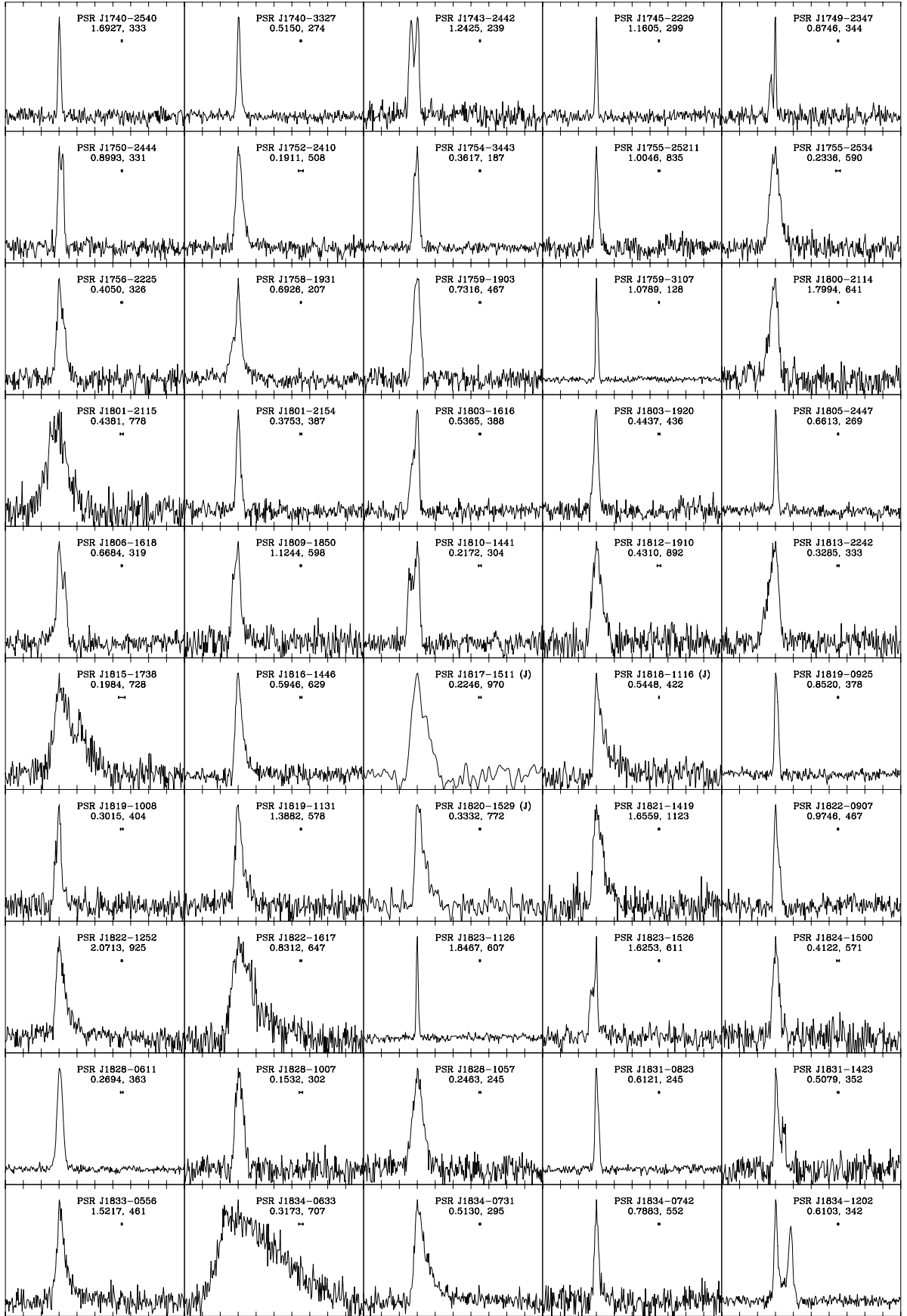
Figure 1 – *continued*
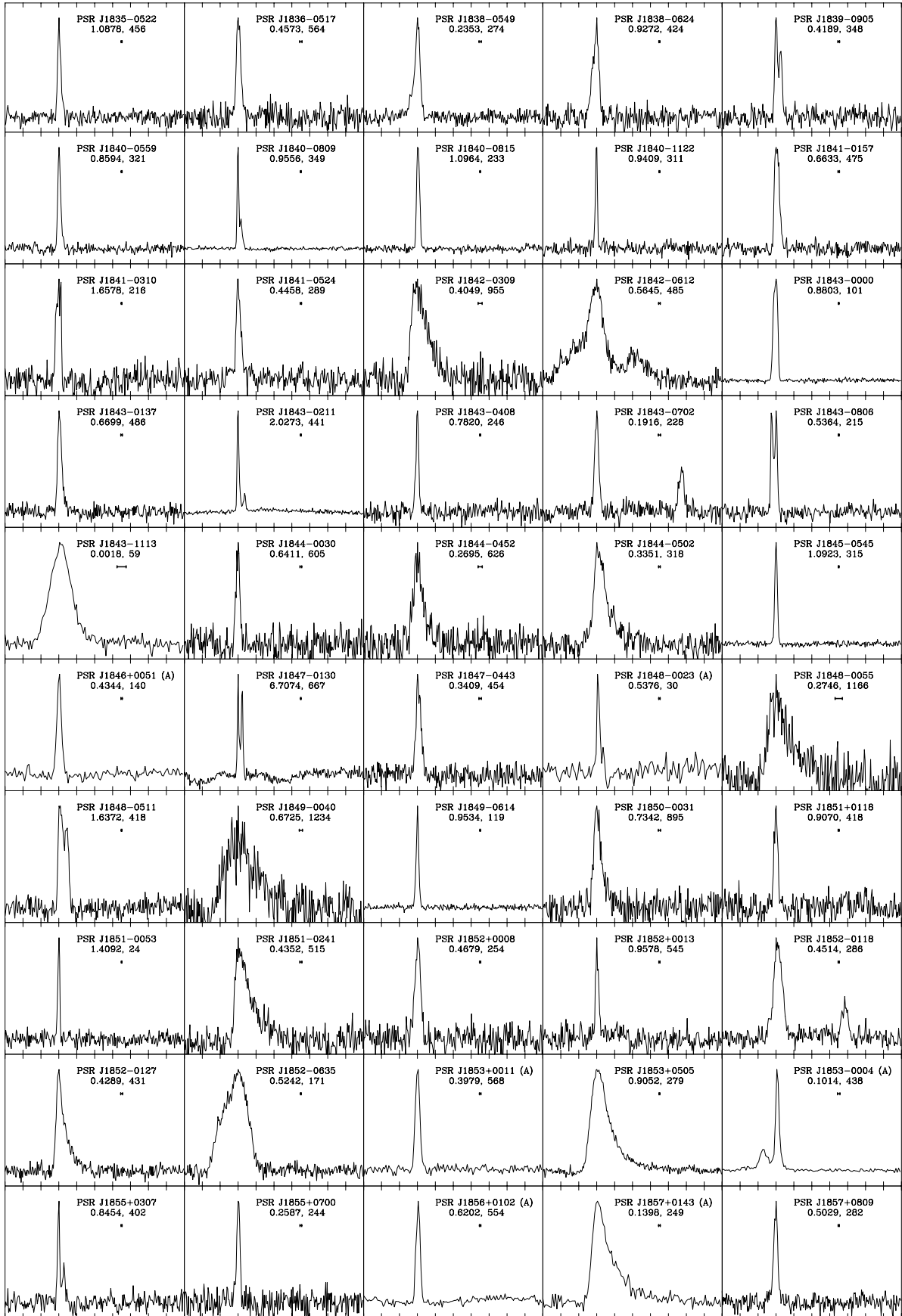
Figure 1 – *continued*

Figure 1 – *continued*

solitary millisecond pulsars are less luminous than those in binary systems. This result was confirmed by Kramer et al. (1998) using a sample of seven isolated millisecond pulsars. The two solitary pulsars, PSRs J1843−1113 and J1905+0400, reported in this paper also have low luminosities at 1400 MHz of 0.39 and 0.09 mJy kpc^2 respectively. The median luminosity at 1400 MHz for the 16 solitary millisecond pulsars known is 0.4 mJy kpc^2 and the luminosity range is from 0.03 mJy kpc^2 for PSR J0030+0451 to 207 mJy kpc^2 for PSR B1937+21. 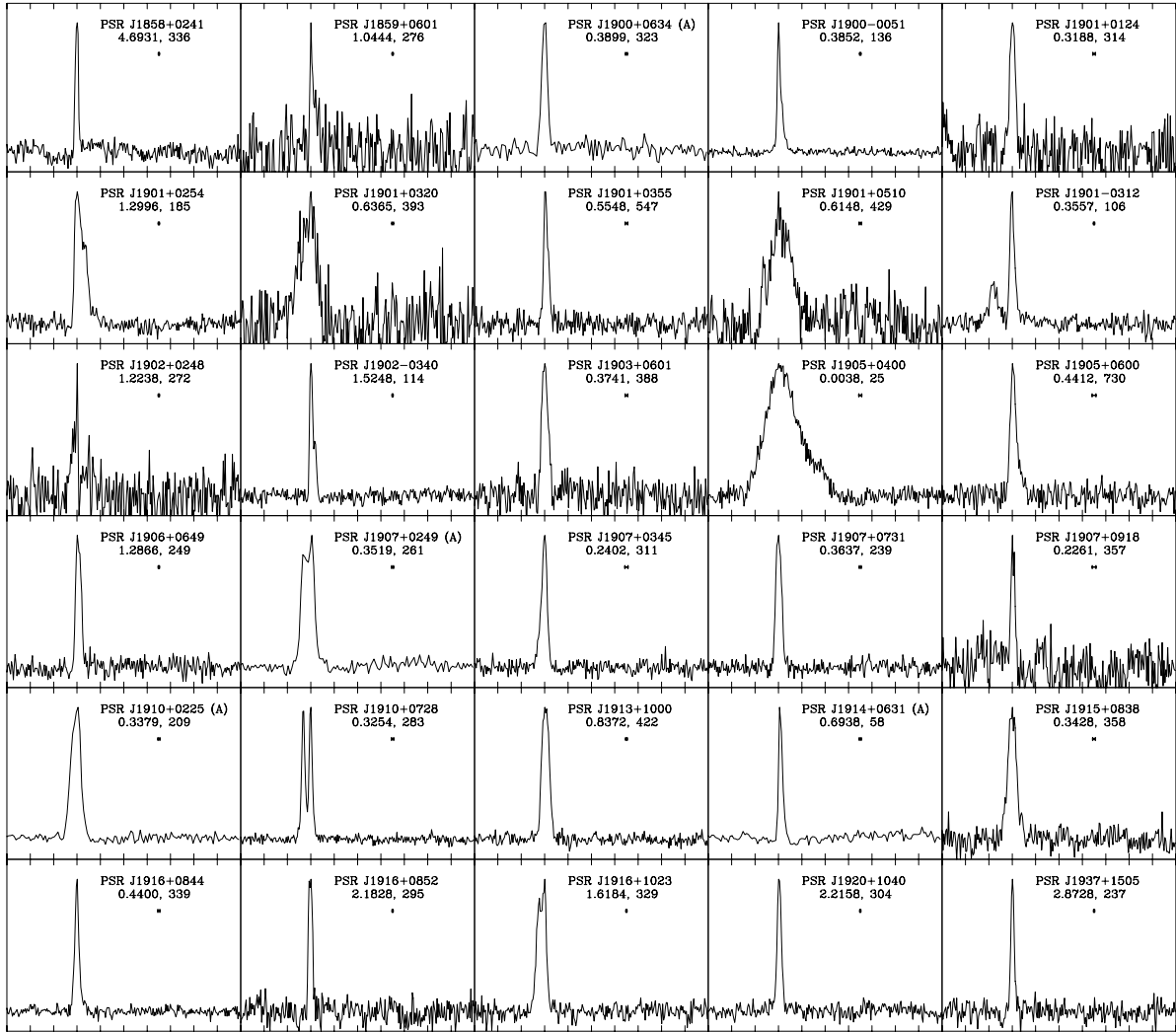The corresponding luminosities for millisecond pulsars in binary systems range between 0.39 and 126 mJy kpc^2 and have a median value of 3.7 mJy kpc^2. We must, however, emphasize that

(i) the fastest rotating and solitary pulsar, PSR B1937+21, has the highest observed luminosity of all the recycled pulsars;

(ii) derived luminosities are highly dependent upon the distance to the pulsar and therefore have large uncertainties; and

(iii) many millisecond pulsars scintillate and therefore published flux densities may not give a true representation of the intrinsic luminosity of the pulsar.

The three millisecond pulsar discoveries all have implications for high-precision pulsar timing and its applications. For instance, observations of PSR B1937+21 have been used to place limits on the gravitational wave background (Lommen 2002). The three discoveries are all well out of the ecliptic plane and have moderate dispersion measures (from 26 cm^{-3} pc for PSR J1905+0400 to 64.9 cm^{-3} pc for the binary system PSR J1420−5625). A figure of merit for precision timing measurement is the ratio $S/W^{3/2}$ where W is the pulse width and S the flux density. However, because of their low flux densities, these three discoveries have lower figures of merit than some other millisecond pulsars such as PSRs B1937+21 and J0437−4715, but they still may be useful as part of a millisecond pulsar timing array. PSR J1843−1113 has been observed at the Parkes observatory using a filterbank with a channel bandwidth of 0.5 MHz and a sampling time of 80 μs. In a typical 10-min observation, signal-to-noise ratios of 10 and uncertainties in the arrival times between 3 and 8 μs have been achieved. It should also be possible to decrease the uncertainties in the arrival times with improved instrumentation.

3.1.2 PSR J1420−5625

The binary system PSR J1420−5625 has a rotational period of 34 ms, a companion mass >0.4 M$_\odot$, a relatively large orbital eccentricity of $e = 0.0035$ and an orbital period of ∼40 d (Table 3). We

Table 2. Periods, period derivatives and dispersion measures for 180 pulsars discovered in the Parkes multibeam pulsar survey. We also give the MJD of the epoch used for period determination, the number of TOAs included in the timing solution, the MJD range covered and the rms of the post-fit timing residuals. Asterisks indicate those pulsars which exhibit significant timing noise that has been removed, to first order, by the fitting of a frequency second derivative (even higher derivatives were included in the timing model if necessary). A superscript '*G*' indicates pulsars that have glitched. A [†] symbol indicates timing solutions already published; see text.

PSR J	Period, P (s)	$\dot{P}$ (10^{-15})	Epoch (MJD)	N_{toa}	Data span (MJD)	Residual (ms)	DM (cm^{-3} pc)
0843−5022[†]	0.2089556931527(14)	0.17238(14)	51500.0	—	51060−51888	—	178.47(9)
1016−5857^{G*}	0.1073864584588(15)	80.8342(6)	52717.0	20	52571−52862	2.87	394.2(2)
1021−5601	0.67002629761(14)	0.053(6)	51875.0	26	51632−52465	3.73	212(8)
1032−5206	2.40762231135(12)	17.891(11)	52161.0	28	51744−52577	1.97	139(4)
1052−6348	0.383830423532(15)	0.387(6)	52477.0	30	52260−52692	0.65	167.5(14)
1054−6452	1.8400035414(3)	3.14(5)	51875.0	23	51632−52118	1.97	234(4)
1055−6022	0.9475584093(3)	92.39(12)	52746.0	23	52569−52923	2.83	590(5)
1106−6438	2.7179341360(3)	2.33(7)	51875.0	23	51632−52118	1.42	203(3)
1152−5800	1.7898294664(5)	1.3(3)	52746.0	21	52569−52923	3.46	191(7)
1156−5707	0.288409420325(8)	26.451(5)	52149.0	23	51944−52352	0.57	243.5(6)
1210−6550	4.2370102164(18)	0.43(11)	52499.0	20	52305−52893	2.89	37(6)
1337−6306	0.207953012189(4)	0.3558(3)	51900.0	95	51220−52578	1.86	777.7(17)
1352−6803	0.628902611443(12)	1.2380(16)	52260.0	28	51944−52574	0.56	215.1(11)
1415−6621[†]	0.39247897310(5)	0.5800(10)	51396.2	—	51569−52151	—	260.17(7)
1420−5625	0.03411713084786(12)	0.000068(17)	52558.0	57	52293−52853	0.07	64.56(9)
1424−5556	0.770374845874(18)	0.780(3)	52260.0	31	51945−52574	0.75	198.7(20)
1435−5954	0.472995435514(16)	1.5433(7)	50545.0	82	49955−51134	0.10	44.26(11)
1437−6146^{G*}	0.46761632345(7)	6.3304(9)	51614.0	56	51710−52883	2.42	200.5(13)
1502−5653	0.535504397790(3)	1.8286(3)	51780.0	30	51214−52345	0.29	194.0(4)
1519−6308	1.25405163056(10)	5.96(5)	52144.0	19	51945−52342	1.49	250(3)
1538−5551	0.104674920844(4)	3.2082(4)	51886.0	42	51466−52305	1.38	603(3)
1542−5133	1.7838649877(3)	0.59(6)	51911.0	26	51634−52187	3.17	186(4)
1547−5750	0.64719774666(6)	0.026(5)	52044.0	17	51744−52342	1.26	148(4)
1551−5310*	0.453394164640(11)	195.1299(9)	52204.0	71	51555−52852	2.68	493(2)
1609−4616	0.249608954839(5)	0.501(4)	52133.0	29	51945−52319	0.40	150.1(6)
1620−5414	1.15636028782(9)	0.067(3)	51830.0	16	51466−52923	1.98	71(8)
1632−4509	1.0468098769(4)	14.88(9)	51973.0	13	51744−52201	1.59	412(4)
1632−4757	0.228564097816(10)	15.0749(10)	51909.0	42	51467−52350	2.39	578(3)
1638−4417	0.1178015507206(9)	1.60526(12)	52142.0	40	51712−52572	0.53	436.0(7)
1658−4958	0.416873770089(11)	3.856(7)	52146.0	18	51946−52344	0.57	193.4(13)
1700−3919	0.560503533065(16)	0.0050(13)	52025.0	18	51495−52596	0.79	354.3(18)
1702−4217	0.227564958458(7)	0.0114(6)	51895.0	29	51216−52572	1.93	629(5)
1708−4522	1.29783683782(7)	2.612(7)	52158.0	28	51744−52572	2.19	454(3)
1715−4254	0.57374535892(7)	0.876(10)	52278.0	31	51984−52571	4.16	407(9)
1718−3714	1.2893787775(3)	26.21(3)	51799.0	28	51463−52135	6.74	833(21)
1718−3718	3.3782065287(14)	1598.15(8)	51776.0	41	51245−52926	27.33	373(13)
1724−3149	0.94823697410(9)	7.25(4)	51995.0	16	51803−52186	0.99	409(4)
1726−4006	0.88277826565(10)	3.33(4)	52475.0	26	52262−52686	1.96	277(3)
1727−2739	1.29309994235(16)	1.10(3)	52263.0	22	51946−52579	2.21	147(4)
1730−3353	3.2702418032(5)	21.96(4)	51672.0	16	51157−52186	3.36	256(10)
1731−3123	0.75304798900(3)	1.679(3)	51702.0	18	51217−52186	0.89	354(3)
1732−4156	0.323434055969(13)	0.661(6)	51911.0	21	51687−52133	0.91	228.7(15)
1733−3030	0.362051962860(14)	1.6485(11)	51914.0	26	51300−52526	2.03	636(3)
1733−4005	0.561778329077(13)	3.624(3)	52385.0	27	51946−52823	0.94	317.8(11)
1736−2819	1.59241948019(13)	14.921(13)	51716.0	19	51244−52186	2.24	261(11)
1736−2843	6.4450360861(17)	29.99(17)	52344.0	28	52001−52686	7.48	331(10)
1737−3320	0.81627308018(6)	2.251(6)	51887.0	21	51581−52192	1.70	804(5)
1738−2647	0.34959099098(5)	3.153(15)	52359.0	13	52146−52572	0.47	182.2(16)
1738−3107	0.54949769829(13)	0.30(7)	52333.0	28	52134−52532	5.49	735(10)
1738−3316	0.73037251102(5)	0.089(4)	51702.0	24	51217−52186	1.99	273(4)

Table 2 – *continued*

PSR J	Period, P (s)	$\dot{P}$ (10^{-15})	Epoch (MJD)	N_{toa}	Data span (MJD)	Residual (ms)	DM $(cm^{-3}\ pc)$
1740−2540	1.69265634040(9)	1.851(12)	52162.0	27	51746−52578	2.11	333(5)
1740−3327	0.515000656402(14)	3.8978(14)	52189.0	26	51805−52572	0.91	274.1(15)
1743−2442	1.24250830909(11)	0.472(10)	52133.0	30	51687−52579	3.42	239(5)
1745−2229	1.160592538166(19)	2.857(3)	52242.0	17	51632−52851	0.80	299(3)
1749−2347	0.87448588170(4)	2.4236(10)	52055.0	16	51217−52926	1.74	344(4)
1750−2444	0.89937672140(5)	0.264(3)	51835.0	27	51091−52579	3.24	331(4)
1752−2410	0.1910366935341(19)	0.61773(8)	51865.0	33	51159−52571	0.59	508.3(9)
1754−3443	0.361690595821(10)	0.5712(7)	52260.0	21	51947−52572	0.40	187.7(9)
1755−25211	1.00451255339(7)	31.2081(13)	51908.0	22	51244−52926	2.09	835(5)
1755−2534	0.233540625445(9)	11.2061(9)	52188.0	31	51804−52571	1.45	590(3)
1756−2225	0.40498030096(9)	52.691(5)	52360.0	20	52149−52926	3.68	326(4)
1758−1931	0.69255157815(7)	16.92(3)	52353.0	24	52134−52571	1.69	207(5)
1759−1903	0.73150547250(17)	3.07(7)	52003.0	26	51804−52201	2.67	467(4)
1759−3107	1.07895331831(4)	3.769(9)	52608.0	19	52391−52823	0.27	128.6(11)
1800−2114	1.7992724923(7)	0.55(26)	52360.0	21	52149−52571	7.56	641(18)
1801−2115	0.4381131572(4)	0.016(6)	51887.0	22	52134−53032	5.06	778.8(1)
1801−2154	0.375296924221(10)	15.9982(5)	51895.0	25	51218−52571	1.02	387.9(14)
1803−1616	0.536595822673(18)	1.7714(12)	51991.0	26	51410−52571	1.58	388.1(20)
1803−1920	0.443648922251(16)	0.3297(8)	51843.0	24	51159−52527	1.23	436.1(17)
1805−2447	0.661401759025(14)	0.0058(7)	51936.0	28	51300−52571	1.06	269(3)
1806−1618	0.66830920992(5)	0.862(3)	51843.0	24	51159−52527	2.51	319(5)
1809−1850	1.12448108944(17)	10.575(8)	51871.0	26	51214−52527	6.01	598(13)
1810−1441	0.217213500357(4)	0.02387(19)	51874.0	28	51220−52527	0.74	304.9(13)
1812−1910	0.43099098078(6)	37.74(3)	51997.0	12	51804−52190	0.94	892(5)
1813−2242	0.328514216183(15)	0.0478(6)	51843.0	29	51159−52527	1.67	333(3)
1815−1738	0.1984357331818(16)	77.85293(12)	52204.0	39	51584−52823	14.31	728(3)
1816−1446	0.594499815819(18)	1.3261(11)	51969.0	27	51410−52527	1.29	629(4)
1817−1511[J]	0.224603837185(16)	1.4313(9)	52160.0	31	51643−52676	2.79	970(5)
1818−1116[J]	0.54479952470(5)	3.824(6)	52158.0	29	51669−52647	2.58	422(7)
1819−0925[J]	0.852047483505(15)	3.1302(11)	52105.0	34	51563−52647	1.03	378(3)
1819−1008[J]	0.301489849278(7)	1.3209(5)	52182.0	22	51743−52619	0.68	404(3)
1819−1131	1.38813712856(16)	0.761(10)	51874.0	18	51220−52527	3.91	578(13)
1820−1529*[J]	0.333242850831(18)	37.9072(10)	52051.0	21	51643−52857	1.17	772(28)
1821−1419	1.6560095697(9)	894.5(3)	52303.0	19	52077−52527	8.85	1123(16)
1822−0907	0.97470037336(6)	0.355(3)	52267.0	22	51681−52852	2.15	467(5)
1822−1252	2.0710402725(5)	84.76(3)	51809.0	31	51091−52527	15.48	925(25)
1822−1617	0.8311557274(3)	1.885(12)	51932.0	30	51335−52527	11.69	647(19)
1823−1126	1.8465342015(3)	36.52(11)	52331.0	17	52135−52527	1.58	607(3)
1823−1526	1.62540547240(16)	4.52(3)	52267.0	21	52001−52532	2.16	611(5)
1824−1500	0.41222995857(6)	0.758(11)	52265.0	22	52001−52527	3.13	571(6)
1828−0611	0.269414732063(3)	1.4595(3)	52045.0	21	51563−52527	0.28	363.2(5)
1828−1007	0.1531969792414(15)	0.61339(12)	51837.0	17	51091−52582	0.49	302.6(12)
1828−1057	0.246327587410(12)	20.7007(19)	52166.0	29	51805−52527	1.96	245(3)
1831−0823[J]	0.612132963973(15)	0.3091(12)	51763.0	25	51410−52115	0.35	245.9(17)
1831−1423	0.507945195243(13)	1.0947(11)	52109.0	11	51689−52527	0.43	352(3)
1833−0556	1.5215451697(4)	1.28(5)	52166.0	32	51805−52527	8.11	461(13)
1834−0633	0.31731488279(7)	0.60(4)	52333.0	21	52138−52528	2.86	707(9)
1834−0731	0.51297990872(4)	58.20(3)	52323.0	18	52117−52527	1.37	295(3)
1834−0742[J]	0.788353566535(19)	32.4702(9)	52145.0	32	51466−52823	1.47	552(18)
1834−1202	0.610258781957(12)	0.0067(3)	52366.0	14	51026−52582	0.30	342.4(13)

Table 2 – *continued*

PSR J	Period, P (s)	$\dot{P}$ (10^{-15})	Epoch (MJD)	N_{toa}	Data span (MJD)	Residual (ms)	DM (cm^{-3} pc)
1835−0522	1.08774918841(8)	0.47(4)	52331.0	20	52134−52528	1.08	456(4)
1836−0517	0.45724503044(3)	1.3019(11)	52156.0	27	51460−52852	2.51	564(5)
1838−0549	0.235303200419(10)	33.429(6)	52642.0	14	52459−52824	0.47	274(7)
1838−0624	0.92717774151(5)	0.077(4)	51875.0	20	51090−52660	3.31	424(9)
1839−0905	0.418968843399(16)	26.033(3)	52287.0	23	52002−52570	0.99	348(4)
1840−0559	0.85936846681(5)	9.602(9)	52418.0	18	52149−52687	0.76	321.7(14)
1840−0809[J]	0.955672135909(8)	2.3510(5)	52091.0	30	51562−52620	0.27	349.8(8)
1840−0815[J]	1.096439972228(14)	2.4151(9)	52091.0	29	51562−52620	0.61	233.2(12)
1840−1122	0.94096161661(4)	6.409(6)	52287.0	25	52002−52570	0.96	311(3)
1841−0157[J]	0.663321097981(9)	18.0768(5)	52163.0	39	51467−52858	1.26	475(3)
1841−0310	1.6576564582(4)	0.335(9)	52353.0	16	51096−52918	4.47	216(12)
1841−0524	0.44574893108(3)	233.724(10)	52360.0	16	52149−52570	0.79	289(15)
1842−0309	0.40491964372(3)	4.518(4)	52493.0	30	52134−52852	2.92	955(7)
1842−0612	0.56447537999(16)	0.022(9)	52402.0	28	52233−52929	4.90	485(10)
1843−0000[J]	0.88033048188(3)	7.792(4)	51910.0	21	51633−52186	0.47	101.5(8)
1843−0137	0.66987238665(3)	2.468(14)	52490.0	21	52293−52687	0.62	486(3)
1843−0211	2.02752438872(5)	14.44(3)	52608.0	17	52391−52824	0.39	441.7(9)
1843−0408	0.78193369973(7)	2.39(3)	52353.0	21	52135−52570	1.99	246(3)
1843−0702	0.191614063108(3)	2.1402(15)	52608.0	19	52391−52824	0.32	228.1(7)
1843−0806	0.536413665506(9)	17.359(4)	52608.0	17	52390−52824	0.29	215.8(9)
1843−1113	0.0018456662924246(5)	0.00000959(5)	52374.0	36	52041−52852	0.01	59.96(3)
1844−0030[A]	0.64109785122(3)	6.078(8)	52632.0	25	52407−52857	0.86	605(3)
1844−0452	0.26944332141(3)	0.680(6)	52471.0	14	52254−52687	0.89	626(4)
1844−0502	0.33516252825(4)	0.062(12)	52608.0	20	52391−52824	1.34	318(5)
1845−0545	1.09234815284(5)	13.43(3)	52608.0	16	52391−52824	0.51	315.9(12)
1846+0051[A]	0.434372879784(16)	11.226(3)	52554.0	31	52279−52828	0.86	140(3)
1847−0130	6.7070457241(9)	1274.9(3)	52353.0	22	52135−52571	2.08	667(6)
1847−0443	0.340832130441(14)	0.0283(4)	52403.0	24	51090−52660	0.91	454.9(20)
1848−0023[A]	0.53762373255(9)	1.610(18)	52522.0	18	52279−52763	1.89	30.6(1)
1848−0055	0.27455668472(7)	1.35(3)	52353.0	22	52134−52571	4.07	1166(7)
1848−0511	1.6371290072(6)	8.863(11)	52777.0	23	51470−53033	5.12	418(7)
1849−0040[A]	0.67248060717(14)	11.14(4)	52633.0	25	52409−52857	3.18	1234.9(1)
1849−0614	0.95338418817(3)	53.889(6)	52417.0	20	52146−52687	0.63	119.6(12)
1850−0031	0.73418485978(10)	1.263(6)	52015.0	25	51460−52569	4.91	895(8)
1851+0118	0.90697686069(14)	136.705(9)	51936.0	23	51301−52569	5.71	418(7)
1851−0053[A]	1.40906524128(16)	0.87(8)	52585.0	28	52407−52763	1.21	24(4)
1851−0241	0.43519385185(4)	7.963(3)	52300.0	25	51747−52852	2.85	515(5)
1852+0008[A]	0.467894113075(20)	5.679(7)	52584.0	32	52310−52857	0.72	254.9(18)
1852+0013[A]	0.95775094505(5)	14.034(12)	52633.0	38	52408−52857	0.99	545(3)
1852−0118	0.45147285265(3)	1.757(11)	52611.0	18	52396−52824	0.99	286(3)
1852−0127	0.42897892562(3)	5.149(8)	52608.0	21	52390−52824	1.12	431(3)
1852−0635	0.52415088472(14)	14.64(5)	52477.0	18	52265−52687	3.31	171(6)
1853+0011[A]	0.397881893633(12)	33.5381(16)	52554.0	28	52279−52828	0.53	568.8(16)
1853+0505	0.905137156487(5)	1.288(5)	52321.0	21	51817−52825	1.93	279(3)
1853−0004[A]	0.1014357461981(14)	5.5745(5)	52633.0	19	52409−52857	0.19	438.2(8)
1855+0307[A]	0.84534757461(4)	18.110(10)	52632.0	29	52407−52857	0.61	402.5(19)
1855+0700	0.258684648071(7)	0.7516(6)	51991.0	21	51413−52569	1.35	244(4)
1856+0102[A]	0.620217115135(20)	1.222(3)	52568.0	40	52279−52857	0.65	554(3)
1857+0143[A]	0.139760064515(4)	31.1674(12)	52632.0	30	52407−52857	0.65	249(3)
1857+0809	0.502923870516(13)	4.7374(8)	51991.0	26	51413−52569	1.33	282(3)

Table 2 – *continued*

PSR J	Period, P (s)	$\dot{P}$ (10^{-15})	Epoch (MJD)	N_{toa}	Data span (MJD)	Residual (ms)	DM $(\text{cm}^{-3}\,\text{pc})$
1858+0241	4.6932329333(12)	24.32(9)	52111.0	22	51688−52532	5.64	336(15)
1859+0601[A]	1.04431270179(15)	25.51(4)	52503.0	56	52279−52726	1.83	276(7)
1900+0634[A]	0.389869101178(20)	5.125(5)	52554.0	54	52279−52828	1.16	323.4(18)
1900−0051[J]	0.385194094862(6)	0.1421(9)	51912.0	24	51634−52188	0.26	136.8(7)
1901+0124[A]	0.318817259335(11)	3.241(4)	52632.0	29	52407−52857	0.56	314.4(13)
1901+0254	1.2996934495(3)	0.46(11)	52626.0	15	52426−52824	2.09	185(5)
1901+0320[A]	0.63658447822(8)	0.52(3)	52503.0	26	52279−52726	2.48	393(7)
1901+0355	0.55475646483(3)	12.741(10)	52352.0	21	52134−52569	0.92	547(3)
1901+0510[A]	0.61475669408(12)	31.10(4)	52618.0	30	52407−52828	2.89	429(7)
1901−0312	0.355725186569(14)	2.292(6)	52608.0	18	52390−52824	0.53	106.4(11)
1902+0248	1.22377745359(17)	2.41(3)	52554.0	35	52279−52828	2.99	272.0(1)
1902−0340	1.5246721060(4)	2.00(17)	52724.0	18	52532−52916	2.43	114(6)
1903+0601[J]	0.374117028251(5)	19.2039(3)	52146.0	33	51467−52824	0.94	388(3)
1905+0400	0.0037844047875897(12)	0.00000486(6)	52173.0	107	51492−52853	0.04	25.71(6)
1905+0600	0.441209731966(18)	1.1123(10)	52048.0	42	51469−52626	0.86	730.1(19)
1906+0649[A]	1.28656437956(10)	0.152(5)	52317.0	31	51805−52828	1.37	249(4)
1907+0249*[A]	0.351879439822(20)	1.135(4)	52554.0	36	52279−52828	3.59	261(6)
1907+0345	0.240153263208(5)	8.222(3)	51999.0	19	51805−52193	0.35	311.7(9)
1907+0731	0.363676330005(12)	18.416(4)	52352.0	22	52134−52569	0.69	239.8(13)
1907+0918[†]	0.2261071099878(6)	94.2955(4)	51319.0	—	51257−51540	—	357.9(1)
1910+0225[A]	0.337854845269(11)	0.2623(14)	52586.0	33	52315−52857	0.75	209(3)
1910+0728	0.325415321974(3)	8.3062(3)	52187.0	23	51805−52569	0.22	283.7(4)
1913+1000	0.83714819649(5)	16.737(6)	52187.0	17	51805−52569	1.21	422(3)
1914+0631[A]	0.69381120574(5)	0.033(13)	52582.0	39	52335−52828	1.16	58(3)
1915+0838[J]	0.34277679653(4)	1.571(4)	52025.0	24	51743−52306	0.99	358(3)
1916+0844[J]	0.439995272067(8)	2.9009(4)	52018.0	30	51467−52569	0.54	339.4(8)
1916+0852	2.1827459895(6)	13.1(3)	52352.0	15	52134−52569	5.21	295(10)
1916+1023[A]	1.6183389208(8)	0.68(14)	52529.0	24	52294−52763	4.65	329.8(1)
1920+1040*[A]	2.21580173889(20)	6.48(3)	52596.0	38	52335−52857	4.46	304(9)
1937+1505[J]	2.8727736506(7)	5.6(3)	51969.0	19	51743−52194	4.11	237(11)

Table 3. Orbital parameters for PSR J1420−5625 obtained using the Bland-ford & Teukolsky (1976) binary model. The minimum companion mass is calculated by assuming an inclination angle of 90° and a neutron-star mass of 1.35 $M_\odot$.

Orbital period (d)	40.294523(4)
Projected semimajor axis of orbit (lt sec)	29.53977(4)
Eccentricity	0.003500(3)
Epoch of periastron (MJD)	52388.945(6)
Longitude of periastron (degrees)	337.30(5)
Minimum companion mass ($M_\odot$)	0.37

note that the periastron advance, $\dot{\omega}$, is likely to be measurable soon, which would provide a value for the total system mass. As PSR J1420−5625 is a recycled pulsar and the orbital eccentricity of the system is significantly less than that measured for double neutron-star systems, the companion is almost certainly a white dwarf (WD) star. As reviewed in Tauris & van den Heuvel (2003) a pulsar is expected to have (1) a He–WD companion if $M_{\text{WD}} \lesssim 0.45\,M_\odot$, (2) a CO–WD companion if $0.45 \lesssim M_{\text{WD}} \lesssim 0.8\,M_\odot$ or (3) an O–Ne–

Mg WD companion if $0.8 \lesssim M_{\text{WD}} \lesssim 1.4\,M_\odot$. Due to the relatively high lower limit on the companion mass for PSR J1420−5625, it is unlikely that the companion is a He–WD; most likely it is a CO–WD.

Similar binary systems have already been discovered during the multibeam survey and were described by Camilo et al. (2001b). Due to their relatively long millisecond spin periods and/or large orbital eccentricities these pulsars are unlike the more common low-mass binary pulsars (LMBPs) and were thus categorized as being intermediate-mass binary pulsars (IMBPs).[5] PSR J1420−5625 has a similarly large spin period and orbital eccentricity and is therefore also an IMBP, making 14 such systems known (Table 5).

PSR J1420−5625 has the longest orbital period and largest orbital eccentricity of the known IMBPs. Edwards & Bailes (2001) reviewed two plausible scenarios for such binary systems. The first, consisting of massive late case A/early case B mass transfer (Tauris, van den Heuvel & Savonije 2000) where the Roche lobe overflow started before or soon after the termination of hydrogen core burning, is limited to systems with orbital periods greater than a few

---

[5] Camilo et al. (2001b) defined IMBPs as objects that once had intermediate-mass donor stars. This applies to pulsar systems with spin periods between 10 and 200 ms and orbital eccentricities less than 0.01.

Table 4. Derived parameters for 180 pulsars discovered in the Parkes multibeam pulsar survey. We list the characteristic age, the surface dipole magnetic field strength, the loss in rotational energy, the distance derived from the DM and the Taylor & Cordes (1993) model, the inferred z-height and the corresponding radio luminosity at 1400 MHz.

PSR J	log [τ_c(yr)]	log [B_s(G)]	log[$\dot{E}$(erg s^{-1})]	Dist. (kpc)	z (kpc)	Luminosity (mJy kpc^2)
0843−5022	7.28	11.28	32.88	7.7	−0.66	18.3
1016−5857	4.32	12.47	36.41	9.3	−0.31	39.9
1021−5601	8.30	11.28	30.85	4.2	0.07	6.5
1032−5206	6.33	12.82	31.71	4.3	0.39	3.6
1052−6348	7.20	11.59	32.43	5.3	−0.36	3.1
1054−6452	6.97	12.39	31.30	13.5	−1.13	45.8
1055−6022	5.21	12.98	33.63	25.6	−0.29	105.1
1106−6438	7.27	12.40	30.66	7.9	−0.55	11.8
1152−5800	7.34	12.18	30.94	7.9	0.54	7.4
1156−5707	5.24	12.45	34.64	20.4	1.76	79.1
1210−6550	8.19	12.14	29.34	1.6	−0.09	0.4
1337−6306	6.97	11.44	33.20	16.0	−0.19	28.2
1352−6803	6.91	11.95	32.30	14.4	−1.47	140.4
1415−6621	7.03	11.68	32.58	14.4	−1.22	147.2
1420−5625	9.90	9.19	31.83	1.7	0.13	0.4
1424−5556	7.19	11.89	31.83	7.7	0.62	22.6
1435−5954	6.69	11.94	32.76	1.5	0.01	7.7
1437−6146	6.07	12.24	33.38	4.8	−0.12	5.5
1502−5653	6.67	12.00	32.67	4.5	0.12	7.9
1519−6308	6.52	12.44	32.08	17.8	−1.52	101.5
1538−5551	5.71	11.77	35.04	10.4	−0.05	27.0
1542−5133	7.68	12.02	30.61	4.9	0.24	6.4
1547−5750	8.60	11.11	30.57	3.9	−0.18	3.5
1551−5310	4.57	12.98	34.92	7.5	0.09	30.5
1609−4616	6.90	11.55	33.11	4.1	0.29	6.5
1620−5414	8.43	11.45	30.23	1.7	−0.09	0.4
1632−4509	6.05	12.60	32.71	9.1	0.32	13.3
1632−4757	5.38	12.27	34.70	7.0	0.01	14.5
1638−4417	6.06	11.64	34.59	8.5	0.26	15.0
1658−4958	6.23	12.11	33.32	6.3	−0.50	34.1
1700−3919	9.25	10.73	30.04	6.3	0.20	9.2
1702−4217	8.50	10.71	31.58	7.5	−0.04	28.1
1708−4522	6.90	12.27	31.67	30.0	−1.57	198.0
1715−4254	7.02	11.86	32.26	12.6	−0.56	11.1
1718−3714	5.89	12.77	32.68	10.9	0.04	27.2
1718−3718	4.53	13.87	33.20	5.1	0.02	4.7
1724−3149	6.32	12.42	32.53	10.5	0.41	39.7
1726−4006	6.62	12.24	32.28	6.2	−0.29	8.0
1727−2739	7.27	12.08	31.30	3.8	0.26	22.5
1730−3353	6.37	12.93	31.40	4.2	−0.00	6.8
1731−3123	6.85	12.06	32.20	5.3	0.13	8.2
1732−4156	6.89	11.67	32.89	8.8	−0.72	17.0
1733−3030	6.54	11.89	33.15	14.2	0.32	40.2
1733−4005	6.39	12.16	32.91	13.9	−0.95	95.4
1736−2819	6.23	12.69	32.18	4.9	0.17	3.8
1736−2843	6.53	13.15	30.64	5.5	0.17	12.9
1737−3320	6.76	12.14	32.20	14.1	−0.20	69.4
1738−2647	6.25	12.03	33.46	3.9	0.17	6.6
1738−3107	7.47	11.61	31.85	10.8	0.02	30.1
1738−3316	8.12	11.41	30.95	4.6	−0.08	11.4

Table 4 – *continued*

PSR J	log [τ_c(yr)]	log [B_s(G)]	log[$\dot{E}$(erg s^{-1})]	Dist. (kpc)	z (kpc)	Luminosity (mJy kpc^2)
1740−2540	7.16	12.25	31.18	8.3	0.38	10.9
1740−3327	6.32	12.16	33.04	4.7	−0.12	6.7
1743−2442	7.62	11.89	30.99	5.0	0.23	3.4
1745−2229	6.81	12.26	31.86	9.3	0.56	11.2
1749−2347	6.76	12.17	32.15	6.1	0.21	4.8
1750−2444	7.73	11.69	31.15	5.0	0.11	6.8
1752−2410	6.69	11.54	33.54	7.4	0.13	25.9
1754−3443	7.00	11.66	32.68	5.6	−0.45	15.4
1755−25211	5.71	12.75	33.08	11.5	−0.00	22.6
1755−2534	5.52	12.21	34.54	7.2	−0.03	8.9
1756−2225	5.09	12.67	34.49	5.0	0.11	6.3
1758−1931	5.81	12.54	33.30	4.2	0.17	6.8
1759−1903	6.58	12.18	32.49	13.3	0.52	28.3
1759−3107	6.66	12.31	32.08	3.4	−0.22	10.3
1800−2114	7.71	12.00	30.57	11.2	0.21	37.5
1801−2115	8.65	10.92	30.86	-1.0	−0.00	0.2
1801−2154	5.57	12.39	34.08	5.2	0.05	4.8
1803−1616	6.68	11.99	32.65	12.9	0.64	26.6
1803−1920	7.33	11.59	32.18	6.5	0.15	11.3
1805−2447	9.26	10.80	29.90	4.8	−0.14	6.2
1806−1618	7.09	11.89	32.04	6.4	0.25	8.9
1809−1850	6.23	12.54	32.46	7.1	0.04	10.0
1810−1441	8.16	10.86	31.96	5.9	0.21	7.3
1812−1910	5.26	12.61	34.28	11.5	−0.09	29.3
1813−2242	8.04	11.10	31.72	6.8	−0.28	9.7
1815−1738	4.61	12.60	35.59	9.0	−0.04	20.3
1816−1446	6.85	11.95	32.40	9.0	0.13	18.5
1817−1511	6.40	11.76	33.70	11.6	0.08	57.7
1818−1116	6.35	12.16	32.97	10.3	0.37	52.9
1819−0925	6.63	12.22	32.30	11.1	0.51	88.7
1819−1008	6.56	11.81	33.28	10.8	0.44	40.4
1819−1131	7.46	12.02	31.04	12.2	0.35	22.5
1820−1529	5.14	12.56	34.60	9.6	−0.07	56.0
1821−1419	4.47	13.59	33.89	11.9	−0.01	28.5
1822−0907	7.64	11.78	31.18	12.3	0.46	18.2
1822−1252	5.59	13.13	32.58	10.6	0.07	28.1
1822−1617	6.84	12.10	32.11	11.6	−0.24	27.1
1823−1126	5.90	12.92	32.36	8.7	0.14	38.8
1823−1526	6.76	12.44	31.62	9.2	−0.15	39.5
1824−1500	6.94	11.75	32.63	8.3	−0.14	11.0
1828−0611	6.47	11.80	33.46	8.8	0.35	92.1
1828−1007	6.60	11.49	33.83	4.7	0.03	4.7
1828−1057	5.28	12.36	34.74	4.3	−0.00	4.2
1831−0823	7.50	11.64	31.72	4.4	0.04	18.9
1831−1423	6.87	11.88	32.52	8.0	−0.31	12.2
1833−0556	7.27	12.15	31.15	7.4	0.16	10.9
1834−0633	6.92	11.65	32.88	9.4	0.12	24.5
1834−0731	5.15	12.74	34.23	4.8	0.03	22.7
1834−0742	5.59	12.71	33.41	6.9	0.03	16.7
1834−1202	9.16	10.81	30.08	6.3	−0.19	27.6

Table 4 – *continued*

PSR J	log [τ_c(yr)]	log [B_s(G)]	log[$\dot{E}$(erg s^{-1})]	Dist. (kpc)	z (kpc)	Luminosity (mJy kpc^2)
1835−0522	7.56	11.86	31.18	7.1	0.14	11.7
1836−0517	6.75	11.89	32.73	8.1	0.13	9.8
1838−0549	5.05	12.45	35.00	4.7	0.02	6.5
1838−0624	8.28	11.43	30.58	5.8	−0.01	5.4
1839−0905	5.41	12.52	34.15	6.1	−0.17	6.0
1840−0559	6.15	12.46	32.78	5.0	−0.02	7.9
1840−0809	6.81	12.18	32.04	5.8	−0.13	76.6
1840−0815	6.86	12.22	31.86	4.5	−0.10	28.3
1840−1122	6.37	12.39	32.48	8.3	−0.40	9.0
1841−0157	5.76	12.54	33.38	7.3	0.15	42.8
1841−0310	7.89	11.88	30.46	4.5	0.06	3.0
1841−0524	4.48	13.01	35.00	4.9	−0.03	4.8
1842−0309	6.15	12.14	33.43	11.4	0.12	32.5
1842−0612	8.61	11.05	30.68	7.0	−0.11	26.5
1843−0000	6.25	12.42	32.65	2.7	0.08	21.6
1843−0137	6.63	12.11	32.51	7.1	0.14	13.2
1843−0211	6.35	12.74	31.83	6.3	0.08	37.4
1843−0408	6.71	12.14	32.30	4.7	−0.01	3.7
1843−0702	6.15	11.81	34.08	4.6	−0.11	3.6
1843−0806	5.69	12.49	33.64	4.6	−0.15	7.5
1843−1113	9.48	8.13	34.78	2.0	−0.12	0.4
1844−0030	6.22	12.30	32.96	8.7	0.19	31.5
1844−0452	6.80	11.64	33.15	8.1	−0.08	12.3
1844−0502	7.93	11.16	31.81	5.2	−0.07	10.8
1845−0545	6.11	12.59	32.61	5.4	−0.13	13.7
1846+0051	5.79	12.35	33.73	3.2	0.08	3.5
1847−0130	4.92	13.97	32.23	7.6	0.02	19.3
1847−0443	8.28	11.00	31.45	7.6	−0.18	9.2
1848−0023	6.72	11.97	32.61	1.5	0.01	1.4
1848−0055	6.51	11.79	33.41	15.1	0.05	43.6
1848−0511	6.47	12.59	31.90	7.8	−0.23	24.2
1849−0040	5.98	12.44	33.15	20.9	0.07	87.0
1849−0614	5.45	12.86	33.40	2.8	−0.12	4.8
1850−0031	6.96	11.99	32.11	10.0	−0.01	22.9
1851+0118	5.02	13.05	33.86	6.8	0.06	4.6
1851−0053	7.41	12.05	31.08	1.2	−0.01	1.5
1851−0241	5.94	12.27	33.58	7.6	−0.16	11.6
1852+0008	6.12	12.22	33.34	5.1	−0.02	8.1
1852+0013	6.03	12.57	32.80	7.2	−0.02	15.6
1852−0118	6.61	11.95	32.88	5.4	−0.07	10.2
1852−0127	6.12	12.18	33.41	6.4	−0.09	24.0
1852−0635	5.75	12.45	33.60	4.6	−0.27	124.8
1853+0011	5.27	12.57	34.32	7.5	−0.05	16.8
1853+0505	7.05	12.04	31.84	7.5	0.26	85.3
1853−0004	5.46	11.88	35.32	6.6	−0.05	37.7
1855+0307	5.87	12.60	33.08	7.4	0.07	53.8
1855+0700	6.74	11.65	33.23	6.8	0.28	4.7
1856+0102	6.91	11.94	32.30	8.6	−0.10	28.2
1857+0143	4.85	12.32	35.65	5.2	−0.05	19.9
1857+0809	6.23	12.19	33.18	8.7	0.37	10.6

© 2004 RAS, MNRAS **352,** 1439–1472

Table 4 – *continued*

PSR J	log [τ_c(yr)]	log [B_s(G)]	log[$\dot{E}$(erg s^{-1})]	Dist. (kpc)	z (kpc)	Luminosity (mJy kpc^2)
1858+0241	6.49	13.03	30.97	6.5	−0.05	4.2
1859+0601	5.81	12.72	32.94	6.0	0.09	10.7
1900+0634	6.08	12.16	33.53	7.3	0.13	12.8
1900−0051	7.63	11.37	31.99	3.3	−0.14	4.9
1901+0124	6.19	12.01	33.59	7.2	−0.21	15.6
1901+0254	7.66	11.89	30.91	4.0	−0.06	9.0
1901+0320	7.29	11.77	31.90	7.7	−0.08	53.3
1901+0355	5.84	12.43	33.46	10.2	−0.08	15.5
1901+0510	5.50	12.65	33.72	8.5	−0.00	47.3
1901−0312	6.39	11.96	33.30	2.9	−0.18	1.9
1902+0248	6.91	12.24	31.72	6.1	−0.13	6.3
1902−0340	7.08	12.25	31.34	3.1	−0.23	2.2
1903+0601	5.49	12.43	34.15	7.8	0.01	16.0
1905+0400	10.09	8.14	33.54	1.3	−0.03	0.1
1905+0600	6.80	11.85	32.71	18.1	−0.09	137.0
1906+0649	8.13	11.65	30.45	5.1	−0.01	7.7
1907+0249	6.69	11.81	33.00	7.5	−0.30	25.8
1907+0345	5.67	12.15	34.36	8.6	−0.27	12.6
1907+0731	5.50	12.42	34.18	4.9	−0.02	8.4
1907+0918	4.58	12.67	35.51	7.7	0.10	17.1
1910+0225	7.31	11.48	32.43	6.3	−0.34	24.0
1910+0728	5.79	12.22	33.98	6.0	−0.08	31.7
1913+1000	5.90	12.58	33.04	7.9	−0.03	33.0
1914+0631	8.52	11.19	30.59	2.7	−0.10	1.9
1915+0838	6.54	11.87	33.18	8.1	−0.18	19.1
1916+0844	6.38	12.06	33.11	8.0	−0.21	28.0
1916+0852	6.42	12.73	31.70	7.0	−0.18	6.3
1916+1023	7.58	12.03	30.80	6.9	−0.10	17.3
1920+1040	6.73	12.58	31.38	7.2	−0.20	29.5
1937+1505	6.91	12.61	30.97	14.1	−0.73	25.7

days and up to ∼70 d and companions lighter than ∼0.9 M$_\odot$. The second, common envelope evolution on the first or second ascent of the red giant branch, is able to account for the remaining systems. PSR J1420−5625 is well modelled by the first scenario. Edwards & Bailes (2001) noted that there seemed an underdensity of pulsars with orbital periods between 12 and 56 d. PSR J1420−5625 lies within this range and this apparent underdensity may have been due only to the small number of such systems known.

3.2 Previously known pulsars

The survey region contains 264 known radio pulsars not discovered by the multibeam survey; over half of these were found during the second Molonglo survey (Manchester et al. 1978), the Jodrell 'B' survey (Clifton et al. 1992) or the Parkes 20-cm survey (Johnston et al. 1992). We have obtained folded pulse profiles for 249 of these pulsars using the multibeam data. Four pulsars (J1841−0345, J1842−0415, J1844−0310 and J1905+0616) were discovered independently in the multibeam survey and other surveys. Parameters for these pulsars were provided in Morris et al. (2002). The remaining 11 pulsars listed in Table 6 were not detected. This was expected for 10 out of the 11 as these weak pulsars were originally

discovered during long observations of supernova remnants or globular clusters or with the highly sensitive Arecibo telescope. As PSR J1156−5909 was discovered during the Parkes Southern Sky survey, it should have easily been detected in the multibeam survey. However, as reported in D'Amico et al. (1998), PSR J1156−5909 has frequent and deep nulls during which the pulsar is undetectable.

A further 32 previously known pulsars that lie outside the nominal survey region were detected mainly due to

(i) observations that were slightly outside of the survey region;
(ii) early observations that were made in the Galactic longitude range $220° < l < 260°$; and
(iii) bright pulsars being observable many beamwidths away from their actual position.

For the 281 previously known pulsars that were detected during the multibeam survey we list, in Table 7, the name of each pulsar, Galactic position, the beam corresponding to the highest S/N detection of this pulsar, the radial distance from the centre of this beam to the actual position of the pulsar in units of beam radii and the S/N of the pulse profile in this detection. If available, we also provide a previously published value for the dispersion measure and flux density of the pulsar at 1400 MHz to compare with our measurements.
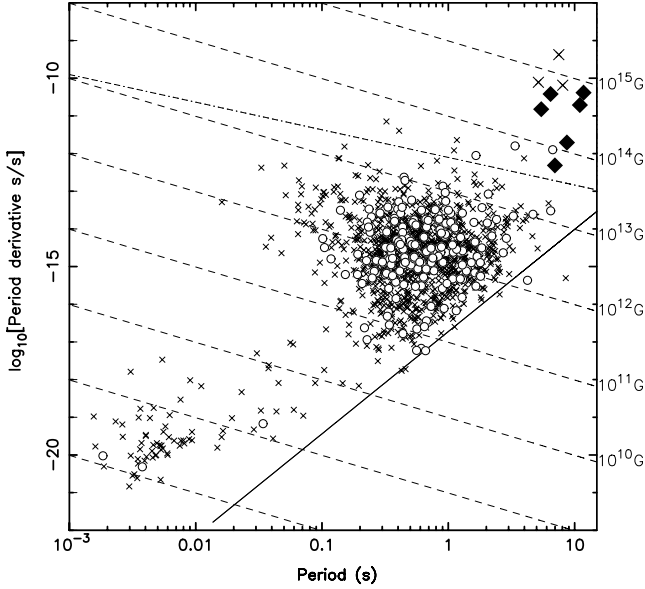
Figure 2. P–$\dot{P}$ diagram containing the multibeam pulsars listed in this paper (circles) overlaid on the previously known population. Diamonds indicate the anomalous X-ray pulsars (AXPs) and large crosses the soft γ-ray repeaters (SGRs) that are listed in the ATNF pulsar catalogue (version 1.13; Manchester et al., in preparation). Lines of constant magnetic field are shown as dashed lines and assume that pulsars, AXPs and SGRs spin down due to magnetic dipole radiation. The AXPs and SGRs lie in a region of the diagram that is predicted to be radio quiet (indicated using a dot-dashed line; and defined by equation 10 in Baring & Harding 2001). The solid line is a 'death-line' defined by $7 \log B_s - 13 \log P = 78$ (Chen & Ruderman 1993).

Table 5. Intermediate-mass binary pulsars (IMBPs) known. The table provides the pulsar's rotational period (P), orbital period (P_b), orbital eccentricity (e) and a lower limit on the companion mass (M_{WD}) assuming a neutron-star mass of $1.35\,M_\odot$.

PSR	P (ms)	P_b (days)	e (10^{-3})	M_{WD} ($M_\odot$)
J0621+1002	28.8	8.3	2.5	>0.44
B0655+64	195.7	1.0	0.0075	>0.66
J1022+1001	16.4	7.8	0.097	>0.71
J1157−5112	43.6	3.5	0.40	>1.18
J1232−6501	88.2	1.9	0.11	>0.14
J1420−5625	34.1	40.3	3.5	>0.37
J1435−6100	9.3	1.4	0.010	>0.88
J1454−5846	45.2	12.4	1.9	>0.86
J1603−7202	14.8	6.3	0.0092	>0.29
J1745−0952	19.4	4.9	0.018	>0.11
J1757−5322	8.9	0.5	0.040	>0.56
J1810−2005	32.8	15.0	0.025	>0.28
J1904+0412	71.0	14.9	0.22	>0.22
J2145−0750	16.0	6.8	0.019	>0.42

The final columns in this table give the pulse width at 50 per cent and 10 per cent of the peak height obtained from the multibeam data.

3.2.1 Flux densities

It is notoriously difficult to obtain flux density measurements that agree with earlier values as

(i) low dispersion measure pulsars scintillate,

(ii) pulsar receiver systems are complex with different systematic biases in different systems,

(iii) the received power is a function of telescope elevation and sky temperature and

(iv) radio-frequency interference (RFI) may significantly affect measured values.

The flux density measurements given in Table 7 were obtained in an identical way to those for the Parkes multibeam discoveries listed in this and previous papers in this series. Full details of the method applied to obtain the flux densities were provided in Manchester et al. (2001). To summarize, the flux densities were calibrated using catalogued 1400-MHz flux densities for 13 pulsars that had high dispersion measures (to minimize variations caused by scintillation). The effect of the varying sky background temperature was determined by scaling the values of the sky background temperature at 408 MHz from the Haslam et al. (1982) all-sky survey to 1374 MHz, assuming a spectral index of −2.5. We correct for off-centre pointing by assuming a Gaussian beam-shape of width 14.4 arcmin. Due to uncertainties in this method, we do not provide flux density measurements for pulsars more than 1.8 beamwidths away from the centre of the beam (this cut-off is chosen as the beam-shape is still reasonably well modelled by a Gaussian up to this approximate distance). The mean pulse profiles at 1374 MHz that were used in determining the flux densities are shown in Fig. 3. The brightest pulsars (indicated with an asterisk in Table 7) saturated the digitizer leading to significantly underestimated flux density measurements and poor pulse profiles. No flux densities or pulse widths are given for these pulsars in Table 7.

In Fig. 4 we compare flux density measurements for all the pulsars with dispersion measures greater than $100\,\mathrm{cm}^{-3}\,\mathrm{pc}$ that are not expected to scintillate strongly. In general, there is good agreement with earlier results. Discrepancies can only be explained by calibration or measurement errors in our or in earlier work. We note that the observing bandwidth of 288 MHz used in these multibeam observations is much larger than that used for previous 20-cm observations. This has the effect of averaging over multiple interference maxima (scintles) and hence lowers the uncertainty in the flux density value due to scintillation effects. Some previous studies have tended to select their best-quality data when determining a flux density. This results in an overestimate of the mean flux density. In any case, the sample of flux densities provided here was obtained using identical on-line and off-line systems and software as the published results for the multibeam survey discoveries. This leads to a sample of almost 1000 pulsars whose flux densities have been measured in an identical way.

For the 38 pulsars listed in Table 8 we have obtained the first flux density measurement at 20 cm. As flux density measurements at other observing frequencies exist in the literature, it is possible to determine the spectral indices of these pulsars. These spectral indices range from −3.3 for PSR B0826−34 to −0.3 for PSR B1804+12 and lie well within the range of −3.4 to 0.2 found by Lorimer et al. (1995). The mean spectral index of −1.9 is, however, slightly steeper than −1.6 found in the earlier analysis. Discrepancies do, however, exist. For instance, Lorimer et al. (1995) measured spectral indices of −1.4 and −0.7 for PSRs B1813−26 and B1907+03, respectively, compared to the steeper values of −2.2 and −2.1 obtained with our data. The spectra for these two pulsars steepen at higher frequencies, an effect commonly observed in other pulsars (Maron et al. 2000).

Table 6. Known pulsars that lie within the Parkes multibeam survey region that were not detected.

PSR J	PSR B	l (°)	b (°)	DM (cm^{-3} pc)	Discovery telescope	S_{1400} (mJy)	Discovery reference
J1124−5916	—	292.04	+1.75	330	Parkes	0.08	Camilo et al. (2002b)
J1156−5909	—	295.91	+2.97	219	Parkes	—	Lyne et al. (1998)
J1617−5055	—	332.50	−0.28	467	Parkes	—	Kaspi et al. (1998)
J1747−2958	—	359.30	−0.84	102	Parkes	0.25	Camilo et al. (2002a)
J1800−2343	B1757−23	6.13	−0.12	280	Ooty	—	Mohanty (1983)
J1817−2311	B1814−23	8.49	−3.27	240	Ooty	—	Mohanty (1983)
J1901+1306	—	45.79	+3.68	75	Arecibo	—	Nice, Fruchter & Taylor (1995)
J1907+1247	B1904+12	46.10	+2.37	257	Arecibo	—	Hulse & Taylor (1975)
J1909+1450	—	48.18	+2.83	120	Arecibo	—	Nice et al. (1995)
J1910+0004	B1908+00	35.17	−4.18	202	Arecibo	—	Deich et al. (1993)
J1918+1541	—	49.89	+1.36	13	Arecibo	—	Nice et al. (1995)

Table 7. Results for 281 previously known pulsars. Catalogued and new dispersion measures and flux densities are provided along with new pulse widths. An asterisk indicates pulsars that saturated the digitizer; for these no flux densities or pulse widths were measured. The pulsars PSR J0820−3927 and J0821−4217 were discovered during the Parkes high-latitude survey (Burgay et al., in preparation). The catalogued flux densities and dispersion are taken from 56 different journal articles. Full bibliographic references may be obtained from the ATNF pulsar catalogue, version 1.13 (Manchester et al., in preparation).

PSR J	PSR B	l (°)	b (°)	Beam	Radial distance	S/N	DM^{cat} (cm^{-3} pc)	DM (cm^{-3} pc)	S_{1400}^{cat} (mJy)	S_{1400} (mJy)	W_{50} (ms)	W_{10} (ms)
J0725−1635	—	231.47	−0.33	11	1.0	31.3	98.98(3)	98.7(4)	0.3	0.33(4)	4.1	—
J0729−1836	B0727−18	233.76	−0.34	1	0.6	0.4	61.292(10)	61.4(3)	1.4	1.40(15)	5.9	25
J0742−2822	B0740−28	243.77	−2.44	6	0.4	1494.7	73.758(8)	73.71(17)	15.0	15.0(15)	5.4	8.3
J0820−3927	—	257.26	−1.58	1	1.4	14.4	196.5(1)	197.0(6)	—	0.32(4)	161	—
J0820−4114	B0818−41	258.75	−2.73	13	1.1	0.1	113.4(2)	113.4(8)	5.2	5.2(5)	135	—
J0821−4217	—	259.77	−3.18	8	2.2	8.1	266.5(1)	266.63(19)	—	—	20	—
J0828−3417	B0826−34	253.97	+2.56	4	1.3	12.5	52.9(6)	52.3(8)	0.2	0.25(4)	—	—
J0835−4510*	B0833−45	263.55	−2.79	4	0.8	2624.9	67.99(1)	67.81(8)	1100.0	—	—	—
J0837−4135	B0835−41	260.90	−0.34	8	0.9	1156.3	147.29(7)	147.29(7)	16.0	16.0(16)	8.9	18
J0842−4851	B0840−48	267.18	−4.10	6	0.6	126.2	196.85(8)	196.85(8)	0.6	0.62(7)	8.3	—
J0846−3533	B0844−35	257.19	+4.71	4	0.7	239.1	94.16(11)	94.12(10)	2.7	2.7(3)	22	76
J0857−4424	—	265.46	+0.82	1	0.3	121.5	184.429(4)	184.02(17)	0.9	0.88(10)	9.9	17
J0904−4246	B0903−42	265.07	+2.86	5	0.3	113.1	145.8(5)	145.8(5)	0.6	0.60(7)	21	32
J0905−4536	—	267.24	+1.01	3	0.2	63.8	116.8(2)	182.5(14)	0.8	0.83(9)	35	—
J0905−5127	—	271.63	−2.85	9	1.1	88.4	196.432(4)	196.1(4)	1.1	1.10(12)	9.0	175
J0907−5157	B0905−51	272.15	−3.03	8	0.3	815.7	103.72(6)	103.72(6)	9.3	9.3(9)	13	24
J0908−4913	B0906−49	270.27	−1.02	13	0.3	888.9	180.37(4)	180.37(4)	10.0	10.0(10)	2.8	—
J0924−5302	B0922−52	274.71	−1.93	7	0.8	131.0	152.9(5)	153.5(4)	1.1	1.10(12)	15	25
J0924−5814	B0923−58	278.39	−5.60	13	1.3	148.9	57.4(3)	57.4(3)	4.3	4.3(4)	41	80
J0934−5249	B0932−52	275.69	−0.70	8	0.9	124.1	99.4(11)	101.1(15)	1.2	1.20(13)	25	42
J0941−5244	—	276.45	+0.09	5	0.7	36.9	157.94(1)	157.8(7)	0.3	0.28(4)	18	—
J0942−5552	B0940−55	278.57	−2.23	6	1.1	491.3	180.2(5)	179.8(3)	10.0	10.0(10)	11	49
J0942−5657	B0941−56	279.35	−2.99	13	0.5	135.8	159.74(12)	159.74(12)	0.7	0.72(8)	7.0	16
J0955−5304	B0953−52	278.26	+1.16	12	1.1	71.3	156.9(2)	156.8(3)	0.9	0.94(10)	7.8	33
J1001−5507	B0959−54	280.23	+0.08	3	0.8	754.1	130.32(17)	130.32(17)	6.3	6.3(6)	15	31
J1012−5857	B1011−58	283.71	−2.14	2	1.0	129.5	383.9(1)	383.13(20)	1.7	1.70(18)	10	23
J1016−5345	B1014−53	281.20	+2.45	2	1.4	47.8	66.8(18)	67.0(4)	0.8	0.82(9)	8.7	17
J1017−5621	B1015−56	282.73	+0.34	9	0.4	156.5	439.1(9)	438.7(5)	2.9	2.9(3)	7.3	—
J1032−5911	B1030−58	285.91	−0.98	4	0.3	130.6	418.20(17)	418.20(17)	0.9	0.93(10)	7.7	17
J1038−5831	B1036−58	286.28	−0.02	2	0.3	116.4	72.74(3)	72.7(4)	0.8	0.79(9)	16	22

Table 7 – *continued*

PSR J	PSR B	l (°)	b (°)	Beam	Radial distance	S/N	DM^{cat} (cm^{-3} pc)	DM (cm^{-3} pc)	S^{cat}_{1400} (mJy)	S_{1400} (mJy)	W_{50} (ms)	W_{10} (ms)
J1042−5521	B1039−55	285.19	+3.00	13	0.1	118.7	306.5(4)	306.5(4)	0.6	0.62(7)	25	39
J1046−5813	B1044−57	287.07	+0.73	5	0.9	93.9	240.2(5)	239.9(6)	1.1	1.10(12)	9.1	16
J1048−5832	B1046−58	287.42	+0.58	12	0.7	536.7	129.1(2)	129.2(5)	6.5	6.5(7)	5.6	9.7
J1056−6258	B1054−62	290.29	−2.97	12	1.0	821.6	320.3(6)	320.11(18)	21.0	21(2)	20	39
J1059−5742	B1056−57	288.34	+1.95	8	0.4	204.8	108.7(3)	108.7(3)	1.2	1.20(13)	18	34
J1104−6103	—	290.33	−0.83	1	0.9	19.2	78.506(15)	78.4(3)	0.2	0.24(3)	4.9	—
J1105−6107	—	290.49	−0.85	4	0.4	56.6	271.01(2)	270.43(4)	0.8	0.75(8)	4.8	—
J1107−5947	B1105−59	290.25	+0.52	12	1.2	23.7	158.4(11)	158.4(11)	0.4	0.43(5)	—	—
J1110−5637	B1107−56	289.28	+3.53	13	0.9	160.2	262.56(6)	262.0(3)	1.8	1.80(19)	22	28
J1112−6613	B1110−65	293.19	−5.23	8	1.9	31.4	249.3(10)	249.5(5)	2.6	—	15	—
J1114−6100	B1112−60	291.44	−0.32	12	1.1	67.6	677.0(4)	677.0(4)	2.0	2.0(2)	29	60
J1121−5444	B1119−54	290.08	+5.87	5	0.4	175.1	204.7(6)	204.5(3)	1.3	1.30(14)	21	27
J1123−6259	—	293.18	−1.78	6	0.6	61.7	223.26(3)	223.14(9)	0.6	0.56(7)	6.6	15
J1123−6651	—	294.47	−5.44	7	1.5	12.1	111.196(5)	111.19(9)	0.4	0.36(5)	—	—
J1126−6054	B1124−60	292.83	+0.29	1	1.1	64.1	280.27(3)	280.25(14)	1.0	1.00(11)	5.1	105
J1133−6250	B1131−62	294.21	−1.30	12	0.9	152.9	567.8(5)	568.6(11)	2.9	2.9(3)	255	305
J1137−6700	—	295.79	−5.17	1	0.8	59.5	228.041(9)	227.4(5)	1.2	1.20(13)	89	—
J1146−6030	B1143−60	294.98	+1.34	10	0.8	318.0	111.68(7)	111.68(7)	3.6	3.6(4)	11	15
J1157−6224	B1154−62	296.71	−0.20	12	0.3	394.8	325.2(5)	324.4(3)	5.9	5.9(6)	13	47
J1202−5820	B1159−58	296.53	+3.92	4	1.2	169.9	145.41(19)	145.41(19)	2.0	2.0(2)	10	16
J1224−6407	B1221−63	299.98	−1.41	4	0.4	548.6	97.47(12)	97.47(12)	3.9	3.9(4)	6.1	9.1
J1225−6408	B1222−63	300.13	−1.41	8	0.2	49.2	415.1(5)	415.1(5)	0.4	0.38(5)	8.1	—
J1239−6832	B1236−68	301.88	−5.69	7	0.2	192.5	94.3(3)	94.3(3)	1.0	0.96(11)	20	40
J1243−6423	B1240−64	302.05	−1.53	13	0.7	1466.0	297.25(8)	297.25(8)	13.0	13.0(13)	6.6	11
J1253−5820	—	303.20	+4.53	7	1.1	245.7	100.584(4)	100.53(12)	3.5	3.5(4)	4.4	13
J1259−6741	B1256−67	303.69	−4.83	8	1.9	13.4	94.7(9)	94.7(9)	1.3	—	—	—
J1302−63	—	304.11	−0.90	5	1.0	10.7	875(10)	874(17)	0.1	0.10(2)	7	—
J1302−6350	B1259−63	304.18	−0.99	5	0.4	124.2	146.72(3)	146.68(8)	1.7	1.70(18)	23	—
J1305−6455	B1302−64	304.41	−2.09	10	1.0	86.4	505.0(3)	505.0(3)	1.6	1.60(17)	19	50
J1306−6617	B1303−66	304.46	−3.46	13	0.9	130.4	436.9(2)	437.6(3)	2.5	2.5(3)	23	59
J1316−6232	—	305.85	+0.19	9	0.9	33.5	983.3(5)	983.3(5)	0.7	0.74(8)	—	—
J1319−6056	B1316−60	306.31	+1.74	4	1.0	94.6	400.94(4)	400.7(3)	1.2	1.20(13)	6.9	15
J1326−5859	B1323−58	307.50	+3.56	12	0.6	867.2	287.30(15)	287.30(15)	9.9	9.9(10)	7.6	23
J1326−6408	B1323−63	306.75	−1.53	3	0.7	133.0	502.7(4)	502.7(4)	1.4	1.40(15)	11	46
J1326−6700	B1322−66	306.31	−4.37	3	0.5	725.5	209.6(3)	209.6(3)	11.0	11.0(11)	42	56
J1327−6222	B1323−62	307.07	+0.20	10	0.9	588.9	318.80(6)	318.80(6)	16.0	16.0(16)	11	19
J1327−6301	B1323−627	306.97	−0.43	5	0.7	180.1	294.91(3)	294.53(8)	3.2	3.2(3)	6.7	30
J1334−5839	—	308.52	+3.75	1	0.8	55.4	119.2978(9)	119.36(7)	0.6	0.62(7)	4.1	—
J1338−6204	B1334−61	308.37	+0.31	9	0.7	199.8	640.3(7)	640.3(7)	3.8	3.8(4)	93	145
J1340−6456	B1336−64	308.05	−2.56	12	1.0	65.7	76.99(13)	76.99(13)	1.1	1.10(12)	14	—
J1341−6220	B1338−62	308.73	−0.03	8	0.8	78.8	717.3(6)	717.9(4)	1.9	1.9(2)	12	41
J1356−6230	B1353−62	310.41	−0.58	11	0.3	535.2	417.3(3)	416.8(4)	8.7	8.7(9)	20	42
J1359−6038	B1356−60	311.24	+1.13	11	0.6	446.5	293.71(14)	293.71(14)	7.6	7.6(8)	3.9	7.4
J1401−6357	B1358−63	310.57	−2.14	10	1.3	300.7	98.0(5)	97.4(3)	6.2	6.2(6)	10	19
J1413−6307	B1409−62	312.05	−1.72	11	1.0	83.7	121.98(6)	121.82(18)	0.9	0.90(10)	4.1	9.2
J1428−5530	B1424−55	316.43	+4.80	5	0.6	517.5	82.4(6)	82.1(3)	3.9	3.9(4)	14	25
J1430−6623	B1426−66	312.65	−5.40	6	1.1	634.5	65.3(1)	64.98(10)	8.0	8.0(8)	18	28
J1440−6344	B1436−63	314.65	−3.38	13	0.6	90.0	124.2(5)	130.2(5)	0.8	0.78(9)	9.7	23
J1453−6413	B1449−64	315.73	−4.43	6	0.5	1423.8	71.07(2)	71.24(8)	14.0	14.0(14)	4.4	9.7
J1512−5759	B1508−57	320.77	−0.11	3	0.9	211.2	628.7(2)	627.93(10)	6.0	6.0(6)	7.8	16

Table 7 – *continued*

PSR J	PSR B	l (°)	b (°)	Beam	Radial distance	S/N	DM^{cat} (cm^{-3} pc)	DM (cm^{-3} pc)	S^{cat}_{1400} (mJy)	S_{1400} (mJy)	W_{50} (ms)	W_{10} (ms)
J1513−5908	B1509−58	320.32	−1.16	6	0.6	50.8	252.5(3)	252.5(3)	0.9	0.94(10)	16	—
J1522−5829	B1518−58	321.63	−1.22	7	1.3	159.0	199.9(2)	199.6(8)	4.3	4.3(4)	14	25
J1527−5552	B1523−55	323.64	+0.59	3	1.3	43.3	362.7(8)	362.7(8)	0.8	0.84(9)	17	—
J1534−5334	B1530−53	325.72	+1.94	5	0.6	622.0	24.82(1)	25.55(13)	6.8	6.8(7)	17	66
J1534−5405	B1530−539	325.46	+1.48	12	0.8	73.1	190.82(2)	190.58(10)	1.2	1.20(13)	6.1	21
J1537−49	—	328.74	+5.22	10	0.5	24.2	65.0(3)	65.0(3)	0.3	0.31(4)	—	—
J1539−5626	B1535−56	324.62	−0.81	5	0.8	296.6	175.88(6)	175.88(6)	4.6	4.6(5)	8.8	17
J1542−5034	—	328.57	+3.58	4	0.8	60.7	91.0(6)	91.0(6)	0.6	0.55(7)	7.3	15
J1544−5308	B1541−52	327.27	+1.32	11	0.6	267.0	35.16(7)	35.16(7)	3.6	3.6(4)	4.6	11
J1549−4848	—	330.49	+4.30	7	0.5	64.5	55.983(8)	56.0(3)	0.5	0.47(6)	6.1	—
J1553−5456	B1550−54	327.19	−0.90	4	1.0	52.7	210(7)	232(7)	0.8	0.79(9)	22	—
J1559−5545	B1555−55	327.24	−2.02	4	0.9	74.1	212.9(3)	212.9(3)	0.7	0.72(8)	9.0	24
J1600−5044	B1557−50	330.69	+1.63	3	0.7	912.0	260.56(9)	262.78(11)	17.0	17.0(17)	5.4	11
J1600−5751	B1556−57	325.97	−3.70	1	0.6	112.2	176.55(8)	176.55(8)	1.4	1.40(15)	11	26
J1602−5100	B1558−50	330.69	+1.29	4	1.1	424.4	170.93(7)	170.93(7)	5.7	5.7(6)	7.9	30
J1603−5657	—	326.88	−3.31	13	0.3	101.8	264.07(2)	264.02(16)	0.5	0.53(6)	4.7	13
J1604−4909	B1600−49	332.15	+2.44	5	1.1	311.6	140.8(5)	140.69(10)	5.5	5.5(6)	4.4	13
J1605−5257	B1601−52	329.73	−0.48	5	0.7	543.2	35.1(3)	35.1(3)	13.0	13.0(13)	59	79
J1611−5209	B1607−52	330.92	−0.48	1	1.0	81.8	127.57(5)	127.57(5)	1.2	1.20(13)	2.2	4.1
J1613−4714	B1609−47	334.57	+2.83	1	4.0	161.7	161.2(3)	161.2(3)	1.5	—	9.7	—
J1614−5048	B1610−50	332.21	+0.17	12	0.8	83.8	582.8(3)	582.7(3)	2.4	2.4(3)	11	37
J1615−5537	B1611−55	329.04	−3.46	9	0.6	51.1	124.48(8)	124.1(5)	0.4	0.44(5)	16	23
J1617−4216	—	338.52	+5.92	4	0.9	22.0	163.6(5)	159.94(18)	0.3	0.28(4)	38	—
J1622−4332	—	338.33	+4.34	13	0.6	53.1	230.68(2)	230.5(12)	0.5	0.53(6)	32	—
J1623−4256	B1620−42	338.89	+4.62	8	0.5	122.1	295(5)	286(3)	1.3	1.30(14)	13	29
J1627−4845	—	335.14	+0.15	1	0.5	29.7	557.8(7)	557.8(7)	0.5	0.48(6)	36	—
J1630−4733	B1626−47	336.40	+0.56	13	1.2	71.2	498(5)	498.2(10)	4.0	4.0(4)	76	—
J1633−4453	B1630−44	338.73	+1.98	2	0.4	165.3	474.1(3)	474.1(3)	1.9	1.9(2)	10	25
J1633−5015	B1629−50	334.70	−1.57	12	1.1	252.8	398.41(8)	398.69(16)	5.7	5.7(6)	8.7	19
J1637−4553	B1634−45	338.48	+0.76	5	0.7	73.7	193.23(7)	193.11(11)	1.1	1.10(12)	3.7	62
J1639−4604	B1635−45	338.50	+0.46	5	1.3	22.8	258.91(4)	258.91(4)	0.8	0.78(9)	8.7	—
J1640−4715	B1636−47	337.71	−0.44	4	0.8	41.4	591.7(8)	591.7(8)	1.2	1.20(13)	23	—
J1644−4559*	B1641−45	339.19	−0.19	11	0.3	890.4	478.8(8)	480.7(4)	310.0	—	—	—
J1646−4346	B1643−43	341.11	+0.97	13	1.1	29.4	490.4(3)	490.4(3)	1.0	0.98(11)	13	—
J1651−4246	B1648−42	342.46	+0.92	5	1.0	427.9	482(3)	482(3)	16.0	16.0(16)	110	165
J1651−5222	B1647−52	335.01	−5.17	12	1.0	229.9	179.1(6)	178.6(3)	2.9	2.9(3)	17	24
J1653−3838	B1650−38	345.88	+3.27	10	0.8	107.2	207.2(2)	206.8(4)	1.3	1.30(14)	4.3	15
J1700−3312	—	351.06	+5.49	5	0.3	157.6	166.97(9)	166.7(7)	1.2	1.20(13)	30	50
J1701−3726	B1658−37	347.76	+2.83	6	0.7	258.1	303.4(5)	299.2(8)	2.9	2.9(3)	43	105
J1701−4533	B1657−45	341.36	−2.18	9	0.9	103.7	526.0(6)	526.0(6)	2.5	2.5(3)	21	35
J1703−3241	B1700−32	351.79	+5.39	2	1.1	534.6	110.306(14)	110.13(3)	7.6	7.6(8)	39	50
J1703−4851	—	338.99	−4.51	11	1.2	57.6	150.29(3)	151.4(3)	1.1	1.10(12)	13	56
J1705−3423	—	350.72	+3.98	7	0.8	276.9	146.36(10)	146.30(7)	4.1	4.1(4)	12	21
J1707−4053	B1703−40	345.72	−0.20	11	0.7	276.1	360.0(2)	357.7(5)	7.2	7.2(7)	33	79
J1708−3426	—	351.08	+3.41	6	0.5	156.7	190.7(3)	189.9(3)	1.5	1.50(16)	23	35
J1709−4429	B1706−44	343.10	−2.69	9	0.7	443.3	75.69(5)	75.56(17)	7.3	7.3(7)	6.0	13
J1713−3949	—	347.30	−0.42	6	0.8	10.3	337(3)	338.3(17)	0.3	0.35(4)	12	—
J1717−3425	B1714−34	352.12	+2.02	2	0.3	276.1	585.21(6)	585.21(6)	3.3	3.3(3)	14	31
J1717−4054	B1713−40	346.82	−1.73	8	2.3	183.2	308.5(5)	308.5(5)	54.0	—	15	30
J1719−4006	B1715−40	347.65	−1.53	2	0.8	69.8	386.6(2)	386.80(14)	1.1	1.10(12)	6.7	13

Table 7 – *continued*

PSR J	PSR B	l (°)	b (°)	Beam	Radial distance	S/N	DM^{cat} (cm^{-3} pc)	DM (cm^{-3} pc)	S_{1400}^{cat} (mJy)	S_{1400} (mJy)	W_{50} (ms)	W_{10} (ms)
J1720−2933	B1717−29	356.50	+4.25	3	0.9	160.9	42.64(3)	42.52(10)	2.1	2.1(2)	17	33
J1721−3532	B1718−35	351.69	+0.67	1	0.6	372.8	496.81(16)	496.81(16)	11.0	11.0(11)	26	69
J1722−3207	B1718−32	354.56	+2.53	6	0.7	309.1	126.064(8)	126.2(3)	3.4	3.4(4)	10	20
J1722−3632	B1718−36	350.93	−0.00	8	0.4	92.7	416.2(2)	415.8(5)	1.6	1.60(17)	22	37
J1722−3712	B1719−37	350.49	−0.51	1	1.0	215.3	99.50(4)	99.44(11)	3.2	3.2(3)	4.0	9.0
J1730−2304	—	3.14	+6.02	12	1.2	82.2	9.611(2)	9.608(15)	3.7	3.7(4)	1.1	—
J1730−3350	B1727−33	354.13	+0.09	5	0.9	106.8	260.6(13)	260.6(13)	3.2	3.2(3)	8.6	22
J1732−4128	B1729−41	347.98	−4.46	4	0.8	66.5	195.3(4)	195.3(4)	0.6	0.63(7)	16	24
J1733−2228	B1730−22	4.03	+5.75	11	1.5	50.7	41.14(3)	40.8(10)	2.3	2.3(2)	60	—
J1733−3716	B1730−37	351.58	−2.28	2	0.8	141.5	153.5(3)	153.5(3)	3.4	3.4(4)	6.2	55
J1737−3555	B1734−35	353.17	−2.27	3	0.7	72.8	89.41(4)	89.06(15)	0.7	0.74(8)	6.9	16
J1738−3211	B1735−32	356.47	−0.49	4	0.9	92.6	49.59(4)	49.7(4)	2.8	2.8(3)	12	26
J1739−2903	B1736−29	359.21	+1.06	10	0.8	141.1	138.56(3)	138.5(3)	2.0	2.0(2)	6.7	—
J1739−3131	B1736−31	357.10	−0.22	7	0.3	240.8	599.5(3)	599.5(3)	4.9	4.9(5)	22	63
J1740−3015	B1737−30	358.29	+0.24	3	0.5	503.7	152.14(20)	152.14(20)	6.4	6.4(7)	5.2	12
J1741−3927	B1737−39	350.55	−4.75	3	1.0	332.7	158.5(6)	158.5(5)	4.7	4.7(5)	9.3	24
J1743−3150	B1740−31	357.30	−1.15	3	1.0	113.0	193.05(7)	192.3(5)	1.9	1.9(2)	45	68
J1744−2335	—	4.46	+2.94	7	2.9	48.3	96.66(2)	98.4(11)	0.2	—	26	—
J1745−3040	B1742−30	358.55	−0.96	1	0.7	586.3	88.373(4)	88.46(9)	13.0	13.0(13)	7.8	23
J1748−2021	B1745−20	7.73	+3.80	3	0.8	19.1	220.4(3)	220.0(3)	0.4	0.37(5)	87	—
J1748−2444	—	3.96	+1.56	3	0.4	26.4	207.33(9)	206.6(2)	0.3	0.34(4)	5.2	—
J1748−2446A	B1744−24A	3.84	+1.70	6	1.2	12.9	242.15(4)	242.15(4)	0.6	0.61(7)	—	—
J1749−3002	B1746−30	359.46	−1.24	9	0.3	146.8	509.4(3)	508.7(5)	3.7	3.7(4)	45	88
J1750−3157	B1747−31	357.98	−2.52	2	1.0	56.1	206.34(4)	206.6(11)	1.2	1.20(13)	10	84
J1750−3503	—	355.31	−4.08	13	0.2	49.0	189.35(2)	189.1(4)	0.8	0.79(9)	67	—
J1752−2806	B1749−28	1.54	−0.96	10	0.2	1603.4	50.372(8)	50.45(12)	18.0	18.0(18)	9.1	15
J1753−2501	B1750−24	4.27	+0.51	6	1.0	49.1	676.2(7)	676.2(7)	2.3	2.3(2)	57	—
J1756−2435	B1753−24	5.03	+0.04	7	0.7	108.9	367.1(4)	365.2(5)	2.0	2.0(2)	25	39
J1757−2421	B1754−24	5.28	+0.05	5	0.8	232.1	179.441(12)	178.7(3)	3.9	3.9(4)	15	24
J1759−2205	B1756−22	7.47	+0.81	9	0.3	151.4	177.157(5)	177.02(20)	1.3	1.30(14)	3.9	11
J1759−2922	—	1.20	−2.89	9	1.1	41.3	79.42(6)	79.4(3)	0.6	0.56(7)	10.0	—
J1801−2304	B1758−23	6.84	−0.07	3	1.1	40.1	1073.9(6)	1073.9(6)	2.2	2.2(2)	—	—
J1801−2451	B1757−24	5.25	−0.88	8	1.0	28.3	289.01(4)	289.01(4)	0.8	0.85(9)	9.6	—
J1801−2920	B1758−29	1.44	−3.25	9	0.7	138.1	125.613(14)	125.55(19)	1.8	1.80(19)	52	63
J1803−2137	B1800−21	8.40	+0.15	10	1.0	199.3	233.99(5)	233.8(3)	7.6	7.6(8)	14	43
J1803−2712	B1800−27	3.49	−2.53	1	0.9	59.8	165.5(3)	165.3(3)	1.0	1.00(11)	18	—
J1804−2717	—	3.51	−2.74	6	0.9	28.0	24.674(5)	24.666(11)	0.8	0.78(9)	—	—
J1806−1154	B1804−12	17.14	+4.42	12	0.6	203.9	122.41(5)	122.0(11)	2.6	2.6(3)	32	41
J1807−0847	B1804−08	20.06	+5.59	12	0.8	944.3	112.3802(11)	112.47(11)	15.0	15.0(15)	8.9	13
J1807−2459	—	5.84	−2.20	11	0.7	10.1	134.0(4)	134.0(5)	1.1	1.10(12)	—	—
J1807−2715	B1804−27	3.84	−3.26	10	1.0	39.9	312.98(3)	313.1(4)	0.9	0.91(10)	14	—
J1808−0813	—	20.63	+5.75	5	1.1	119.5	151.27(6)	150.6(6)	1.8	1.80(19)	24	40
J1808−2057	B1805−20	9.45	−0.40	7	0.9	134.6	606.8(9)	607(4)	2.6	2.6(3)	76	—
J1809−0743	—	21.25	+5.67	4	0.1	37.4	240.70(14)	240.8(4)	0.3	0.29(4)	12	—
J1809−2109	B1806−21	9.41	−0.72	5	0.9	58.7	381.91(5)	381.0(4)	0.8	0.84(9)	13	—
J1812−1718	B1809−173	13.11	+0.54	10	1.1	52.0	254.6(4)	254.6(4)	1.0	1.00(11)	19	—
J1812−1733	B1809−176	12.90	+0.39	10	0.6	110.2	518(4)	528(8)	3.3	3.3(3)	63	—
J1816−1729	B1813−17	13.43	−0.42	1	0.9	74.1	525.5(7)	526.6(3)	1.2	1.20(13)	17	34
J1816−2650	B1813−26	5.22	−4.91	2	0.9	67.8	128.12(3)	128.0(5)	1.1	1.10(12)	40	—
J1818−1422	B1815−14	16.41	+0.61	5	0.5	291.9	622.0(4)	621.7(5)	7.1	7.1(7)	19	53

Table 7 – *continued*

PSR J	PSR B	l (°)	b (°)	Beam	Radial distance	S/N	DM^{cat} (cm^{-3} pc)	DM (cm^{-3} pc)	S^{cat}_{1400} (mJy)	S_{1400} (mJy)	W_{50} (ms)	W_{10} (ms)
J1820−0427	B1818−04	25.46	+4.73	3	0.9	562.7	84.435(17)	84.39(8)	6.1	6.1(6)	11	20
J1820−1346	B1817−13	17.16	+0.48	12	0.8	83.7	776.7(17)	779.5(6)	2.0	2.0(2)	33	120
J1820−1818	B1817−18	13.20	−1.72	4	0.9	64.0	436.0(12)	436.6(3)	1.1	1.10(12)	16	—
J1822−1400	B1820−14	17.25	−0.18	4	1.1	24.9	651.1(9)	647.9(6)	0.8	0.80(9)	9.1	—
J1822−2256	B1819−22	9.35	−4.37	8	0.9	209.2	121.20(4)	119(3)	2.4	2.4(3)	46	81
J1823−0154	—	28.08	+5.26	10	1.0	78.1	135.87(5)	136.18(12)	0.8	0.78(9)	8.1	17
J1823−1115	B1820−11	19.77	+0.95	9	0.4	118.9	428.59(9)	428.6(5)	3.2	3.2(3)	26	—
J1824−1118	B1821−11	19.81	+0.74	13	0.6	77.6	603(2)	604(4)	1.3	1.30(14)	23	—
J1824−1945	B1821−19	12.28	−3.11	2	0.8	492.3	224.649(5)	224.452(14)	4.9	4.9(5)	2.9	5.5
J1824−2452	B1821−24	7.80	−5.58	11	0.9	7.7	119.857(7)	120.1(9)	0.2	0.18(3)	—	—
J1825−0935	B1822−09	21.45	+1.32	8	1.1	548.6	19.39(4)	19.33(20)	12.0	12.0(12)	12	42
J1825−1446	B1822−14	16.81	−1.00	5	1.1	83.4	357(5)	353(3)	2.6	2.6(3)	12	27
J1826−1131	B1823−11	19.80	+0.29	7	0.9	48.2	320.58(6)	322(4)	0.7	0.71(8)	160	—
J1826−1334	B1823−13	18.00	−0.69	11	1.2	56.5	231.09(8)	231.09(8)	2.1	2.1(2)	5.8	—
J1827−0958	B1824−10	21.29	+0.80	5	0.3	93.4	430.1(3)	430.1(3)	1.8	1.80(19)	22	—
J1829−1751	B1826−17	14.60	−3.42	5	0.1	724.3	217.109(9)	216.42(9)	7.7	7.7(8)	15	20
J1830−1059	B1828−11	20.81	−0.48	3	0.9	125.4	161.50(15)	159.67(11)	1.4	1.40(15)	3.2	6.3
J1832−0827	B1829−08	23.27	+0.30	9	1.0	126.7	300.853(13)	300.48(4)	2.1	2.1(2)	7.1	25
J1832−1021	B1829−10	21.59	−0.60	5	0.1	118.8	475.7(3)	474.8(4)	1.3	1.30(14)	8.4	18
J1833−0338	B1831−03	27.66	+2.27	1	0.4	303.9	234.537(14)	234.17(16)	2.8	2.8(3)	7.5	23
J1833−0827	B1830−08	23.39	+0.06	3	0.8	113.9	410.925(12)	410.925(12)	3.6	3.6(4)	4.9	15
J1834−0010	B1831−00	30.81	+3.73	10	0.5	18.4	88.65(15)	88.2(4)	0.3	0.29(4)	—	—
J1834−0426	B1831−04	27.04	+1.75	8	1.0	166.3	79.308(8)	79(4)	5.0	5.0(5)	84	99
J1835−0643	B1832−06	25.09	+0.55	10	0.2	68.6	472.9(10)	472.7(3)	1.3	1.30(14)	32	—
J1835−1106	—	21.22	−1.51	13	1.2	95.0	132.679(3)	132.57(10)	2.2	2.2(2)	4.7	9.4
J1836−0436	B1834−04	27.17	+1.13	5	1.2	84.1	231.5(3)	231.3(3)	1.8	1.80(19)	9.1	17
J1836−1008	B1834−10	22.26	−1.42	3	0.2	260.0	316.97(3)	316.1(3)	3.7	3.7(4)	8.7	17
J1837−0045	—	30.67	+2.75	1	1.1	32.1	86.98(9)	87.4(10)	0.6	0.61(7)	9.6	—
J1837−0653	B1834−06	25.19	+0.00	3	0.1	159.2	316.1(4)	315.5(12)	2.5	2.5(3)	105	170
J1837−1837	—	14.81	−5.50	3	0.3	58.3	100.74(13)	100.8(3)	0.4	0.36(5)	9.0	18
J1841−0425	B1838−04	27.82	+0.28	2	0.9	127.0	325.487(15)	325.14(12)	2.6	2.6(3)	5.3	9.9
J1842−0359	B1839−04	28.35	+0.17	7	0.2	213.0	195.98(8)	197.4(18)	4.4	4.4(5)	285	340
J1844+00	—	32.62	+1.88	3	1.2	284.7	345.54(20)	345.54(20)	8.6	8.6(9)	12	43
J1844−0244	B1842−02	29.73	+0.24	1	0.4	63.5	428.5(5)	428.5(5)	0.9	0.87(10)	20	—
J1844−0256	—	29.57	+0.12	4	0.9	14.4	820.2(3)	820.2(3)	0.5	0.46(6)	68	—
J1844−0433	B1841−04	28.10	−0.55	9	0.3	131.2	123.158(20)	123.0(5)	1.1	1.10(12)	13	28
J1844−0538	B1841−05	27.07	−0.94	1	1.1	85.2	412.8(3)	411.0(3)	2.2	2.2(2)	19	—
J1845−0316	—	29.39	−0.26	7	1.1	12.2	500.00(14)	500.00(14)	0.3	0.35(4)	12	—
J1845−0434	B1842−04	28.19	−0.78	12	0.1	174.0	230.8(17)	230.2(17)	1.6	1.60(17)	17	29
J1847−0402	B1844−04	28.88	−0.94	1	0.8	267.9	141.979(5)	141.0(5)	4.3	4.3(4)	22	30
J1848+0647	—	38.70	+3.65	8	0.6	17.0	27.9(2)	25.0(8)	0.2	0.17(3)	13	—
J1848+0826	—	40.15	+4.44	10	0.4	9.5	90.77(7)	90.4(3)	0.1	0.11(2)	—	—
J1848−0123	B1845−01	31.34	+0.04	3	0.7	514.1	159.531(8)	159.96(12)	8.6	8.6(9)	17	37
J1849+06	—	38.12	+3.30	9	1.1	14.6	235(3)	235(3)	0.3	0.35(4)	89	—
J1849−0636	B1846−06	26.77	−2.50	13	0.9	123.4	148.168(12)	148.3(10)	1.4	1.40(15)	89	—
J1850+1335	B1848+13	44.99	+6.34	11	0.7	83.2	60.147(8)	60.0(4)	0.7	0.65(7)	5.7	11
J1851+0418	B1848+04	36.72	+2.05	10	0.9	34.0	115.54(5)	112.01(10)	0.7	0.66(8)	71	—
J1851+1259	B1848+12	44.51	+5.93	4	1.5	43.6	70.615(16)	70.8(10)	0.8	0.75(8)	11	21
J1852+0031	B1849+00	33.52	+0.02	10	0.5	98.6	798.2(16)	798.2(16)	2.2	2.2(2)	235	—
J1854+1050	B1852+10	42.89	+4.22	12	0.3	88.4	207.2(3)	208(12)	1.0	1.03(14)	43	—

Table 7 – *continued*

| PSR J	PSR B	*l* (°)	*b* (°)	Beam	Radial distance	S/N	DM^{cat} (cm^{-3} pc)	DM (cm^{-3} pc)	S_{1400}^{cat} (mJy)	S_{1400} (mJy)	W_{50} (ms)	W_{10} (ms)
J1855−0941	—	24.72	−5.24	8	0.3	39.5	151.99(14)	151.99(14)	0.5	0.48(6)	26	—
J1856+0113	B1853+01	34.56	−0.50	10	0.5	20.8	96.79(10)	96.83(19)	0.2	0.19(3)	3.8	—
J1857+0057	B1854+00	34.42	−0.81	3	0.9	49.8	82.39(11)	83.0(7)	0.9	0.92(10)	22	—
J1857+0212	B1855+02	35.62	−0.39	7	0.7	117.5	506.77(18)	504.2(4)	1.6	1.60(17)	14	23
J1857+0943	B1855+09	42.29	+3.06	2	0.4	240.2	13.309(5)	13.301(4)	4.3	4.3(4)	0.55	3.0
J1859+00	—	34.40	−1.59	7	1.1	163.9	420(3)	420(3)	4.8	4.8(5)	54	97
J1901+00	—	34.47	−2.05	8	0.9	27.8	345.5(11)	345.5(11)	0.3	0.35(4)	22	—
J1901+0156	B1859+01	35.82	−1.37	2	0.4	39.7	105.394(7)	102.8(4)	0.4	0.38(5)	6.1	—
J1901+0331	B1859+03	37.21	−0.64	7	0.2	359.1	402.080(12)	400.82(10)	4.2	4.2(4)	11	36
J1901+0716	B1859+07	40.57	+1.06	7	0.7	74.0	252.81(7)	252.5(5)	0.9	0.90(10)	11	34
J1902+0556	B1900+05	39.50	+0.21	11	0.3	151.0	177.486(13)	177.7(4)	1.2	1.20(13)	11	29
J1902+0615	B1900+06	39.81	+0.34	3	0.8	99.7	502.900(17)	502(3)	1.1	1.10(12)	24	—
J1902+0723	—	40.74	+0.98	7	0.4	16.1	105.0(3)	105.0(4)	0.2	0.17(3)	—	—
J1903+0135	B1900+01	35.73	−1.96	10	1.1	350.3	245.163(6)	244.95(11)	5.5	5.5(6)	9.9	23
J1904+0004	—	34.45	−2.81	9	1.0	96.3	233.61(4)	233.6(3)	2.1	2.1(2)	7.8	22
J1904+1011	B1901+10	43.43	+1.87	7	0.9	26.0	135(2)	136.0(20)	0.6	0.58(7)	28	—
J1905+0709	B1903+07	40.94	+0.07	9	1.0	67.3	245.34(10)	247(13)	1.8	1.80(19)	39	—
J1905−0056	B1902−01	33.69	−3.55	6	1.1	68.3	229.131(5)	228.2(3)	0.9	0.92(10)	6.2	15
J1906+0641	B1904+06	40.60	−0.30	10	1.1	56.5	473.15(4)	473.15(4)	1.7	1.70(18)	18	—
J1908+0457	—	39.27	−1.47	8	0.4	89.2	360(5)	353(3)	0.9	0.93(10)	42	59
J1908+0500	—	39.29	−1.40	8	0.5	89.2	201.42(2)	201.27(17)	0.8	0.79(9)	3.9	7.6
J1908+0734	—	41.58	−0.27	7	0.7	30.9	11.104(11)	11.09(15)	0.5	0.54(6)	2.8	—
J1908+0916	B1906+09	43.17	+0.36	9	0.1	20.0	249.8(5)	249.8(5)	0.2	0.23(3)	26	—
J1909+0007	B1907+00	35.12	−3.98	11	0.8	112.2	112.787(6)	112.65(12)	0.9	0.87(10)	8.0	31
J1909+0254	B1907+02	37.60	−2.71	8	1.3	38.7	171.734(9)	172.4(14)	0.6	0.63(7)	11	—
J1909+1102	B1907+10	44.83	+0.99	1	0.8	182.0	149.982(4)	149.74(14)	1.9	1.9(2)	4.8	13
J1910+0358	B1907+03	38.61	−2.34	12	0.9	51.8	82.93(10)	78.0(8)	1.5	1.50(16)	265	—
J1910+0714	—	41.52	−0.87	11	0.8	39.4	124.06(5)	125.5(15)	0.4	0.36(5)	22	735
J1910+1231	B1907+12	46.20	+1.59	2	0.1	46.8	258.64(12)	257.7(7)	0.3	0.28(4)	18	—
J1910−0309	B1907−03	32.28	−5.68	11	1.0	37.6	205.53(3)	205.13(11)	0.6	0.55(7)	7.6	—
J1912+1036	B1910+10	44.79	+0.15	9	0.9	17.6	147.0(5)	147.0(6)	0.2	0.22(3)	—	—
J1913+0936	B1911+09	44.03	−0.55	3	0.7	14.0	157(2)	156.5(11)	0.1	0.14(2)	—	—
J1913+1400	B1911+13	47.88	+1.59	1	0.5	152.2	145.052(5)	145.0(3)	1.2	1.20(13)	6.2	22
J1914+1122	B1911+11	45.62	+0.20	10	0.3	68.2	100(10)	100(10)	0.6	0.55(7)	25	—
J1915+07	—	42.63	−1.60	1	0.6	36.8	112.5(18)	112.5(18)	0.2	0.21(3)	23	—
J1915+0738	—	42.47	−1.80	7	1.1	37.4	39.00(8)	39.3(6)	0.3	0.34(4)	11	24
J1915+1009	B1913+10	44.71	−0.65	2	0.5	178.7	241.693(10)	241.6(3)	1.3	1.30(14)	6.7	13
J1915+1606	B1913+16	49.97	+2.12	1	0.0	29.7	168.77(1)	168.73(8)	0.4	0.42(5)	7.0	—
J1916+07	—	42.85	−2.02	2	0.8	159.2	305.1(8)	305.1(8)	2.8	2.8(3)	115	—
J1916+0951	B1914+09	44.56	−1.02	11	0.8	57.1	60.953(6)	61.24(19)	0.9	0.91(10)	9.6	—
J1916+1030	B1913+105	45.10	−0.64	1	0.5	22.4	387.2(3)	387.2(3)	0.2	0.22(3)	20	—
J1916+1312	B1914+13	47.58	+0.45	12	0.2	162.2	237.016(11)	236.7(3)	1.2	1.20(13)	6.2	11
J1917+1353	B1915+13	48.26	+0.62	6	0.6	204.6	94.538(4)	94.51(12)	1.9	1.9(2)	4.0	9.1
J1918+08	—	43.71	−2.02	5	0.8	32.2	30(1)	29.8(15)	0.3	0.31(4)	58	—
J1918+1444	B1916+14	49.10	+0.87	3	1.1	79.8	27.202(17)	30.3(13)	1.0	1.00(11)	28	—
J1919+0134	—	37.58	−5.56	10	1.1	40.9	191.9(4)	192.0(7)	0.8	0.77(9)	55	—
J1921+1419	B1919+14	49.06	+0.02	11	0.8	45.8	91.64(4)	91.5(5)	0.7	0.68(8)	22	—
J1926+1434	B1924+14	49.92	−1.04	8	0.9	24.2	211.41(8)	211.1(8)	0.5	0.48(6)	16	—
J1930+1316	B1927+13	49.12	−2.32	13	1.1	11.8	207.3(9)	207.6(4)	0.2	0.18(3)	—	—
J1932+1059	B1929+10	47.38	−3.88	6	0.9	1697.0	3.181(4)	3.3(2)	36.0	36(4)	7.4	14
J1933+1304	B1930+13	49.35	−3.13	7	0.9	37.6	177.9(2)	177.0(6)	0.4	0.42(5)	29	—
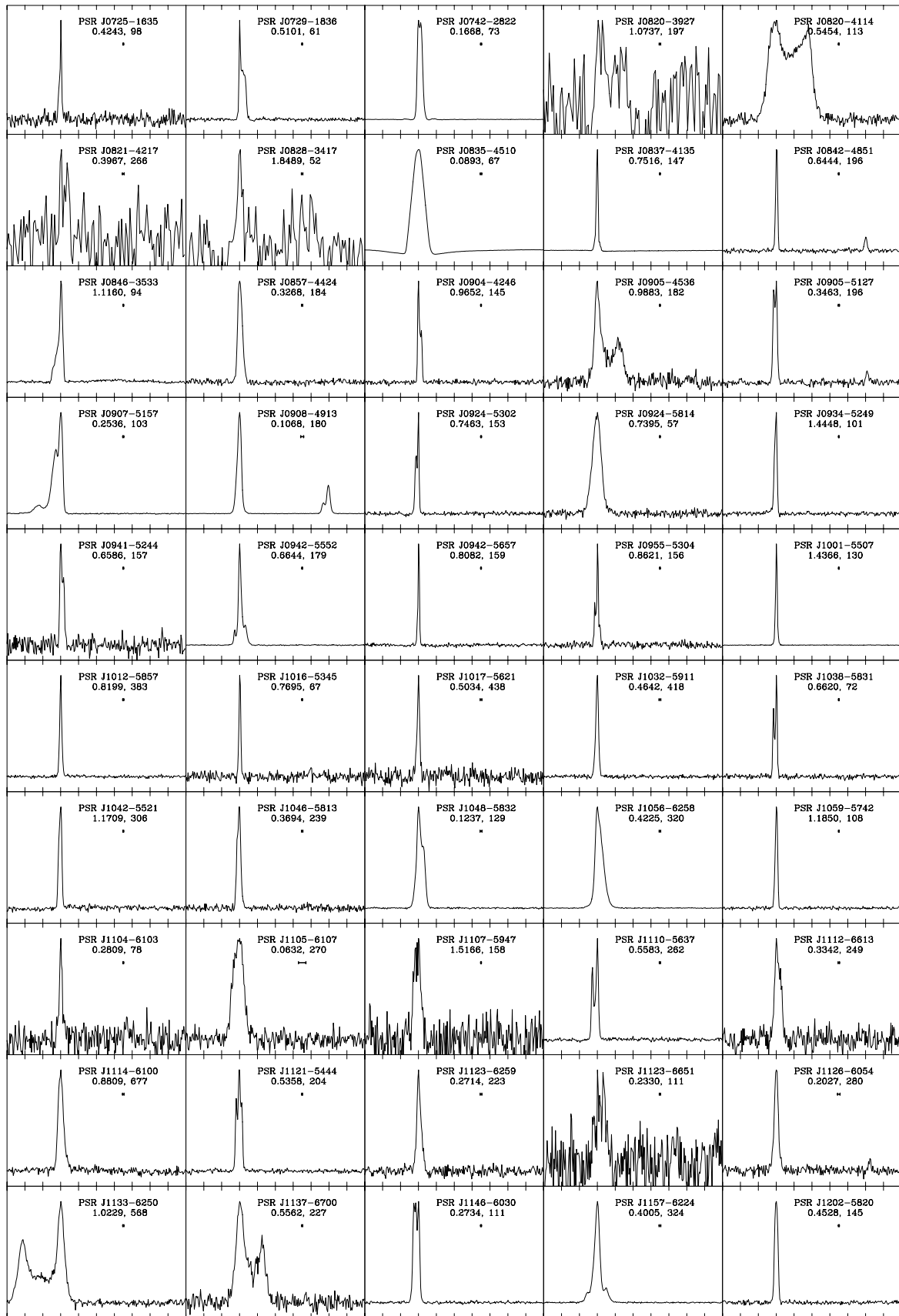
Figure 3. Mean 1374-MHz pulse profiles for 281 pulsars redetected in the Parkes multibeam survey. The highest point in the profile is placed at phase 0.3. For each profile, the pulsar Jname, pulse period (s) and dispersion measure (cm^{-3} pc) are given. The small horizontal bar under the period indicates the effective resolution of the profile by adding the bin size to the effects of interstellar dispersion in quadrature.
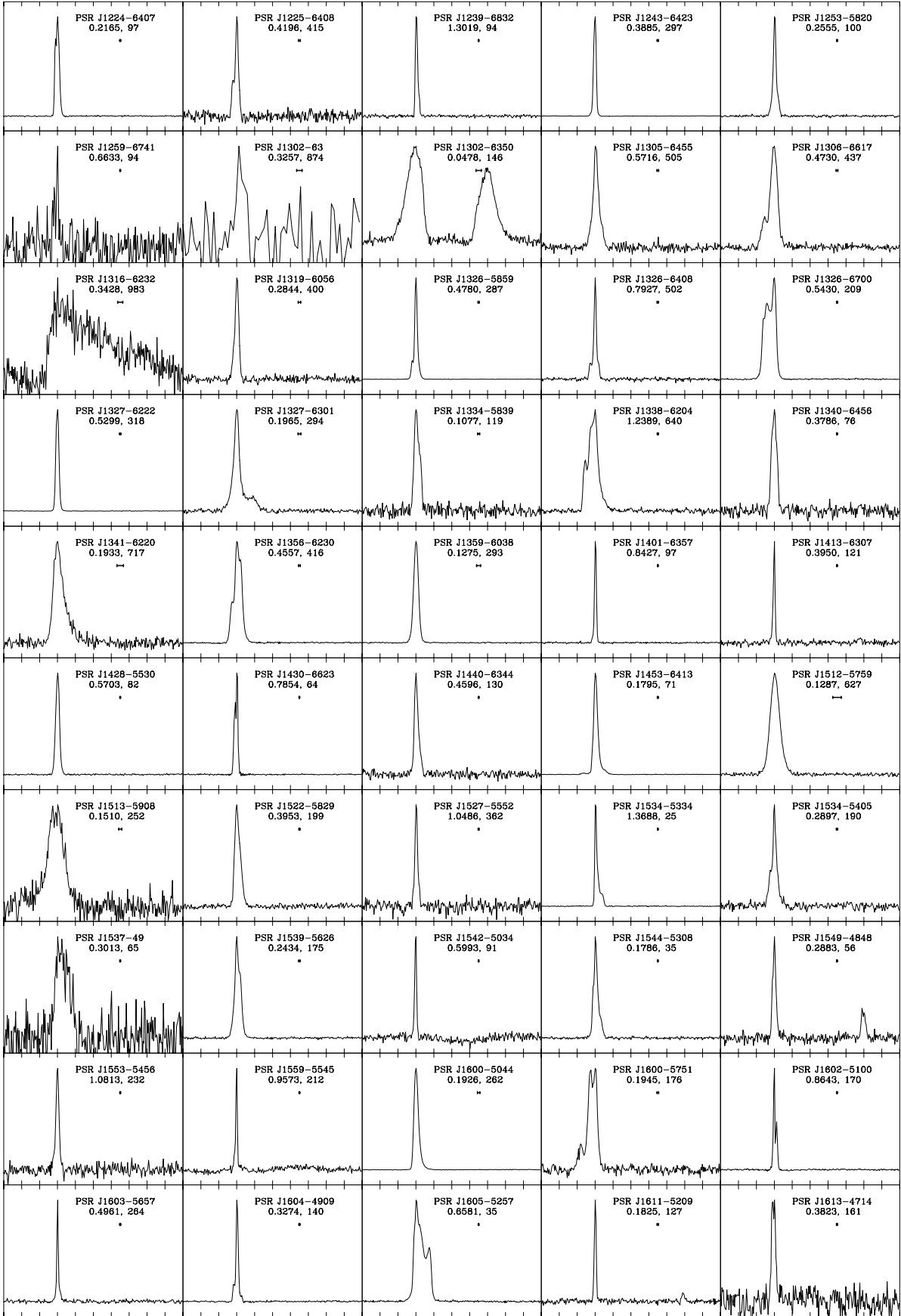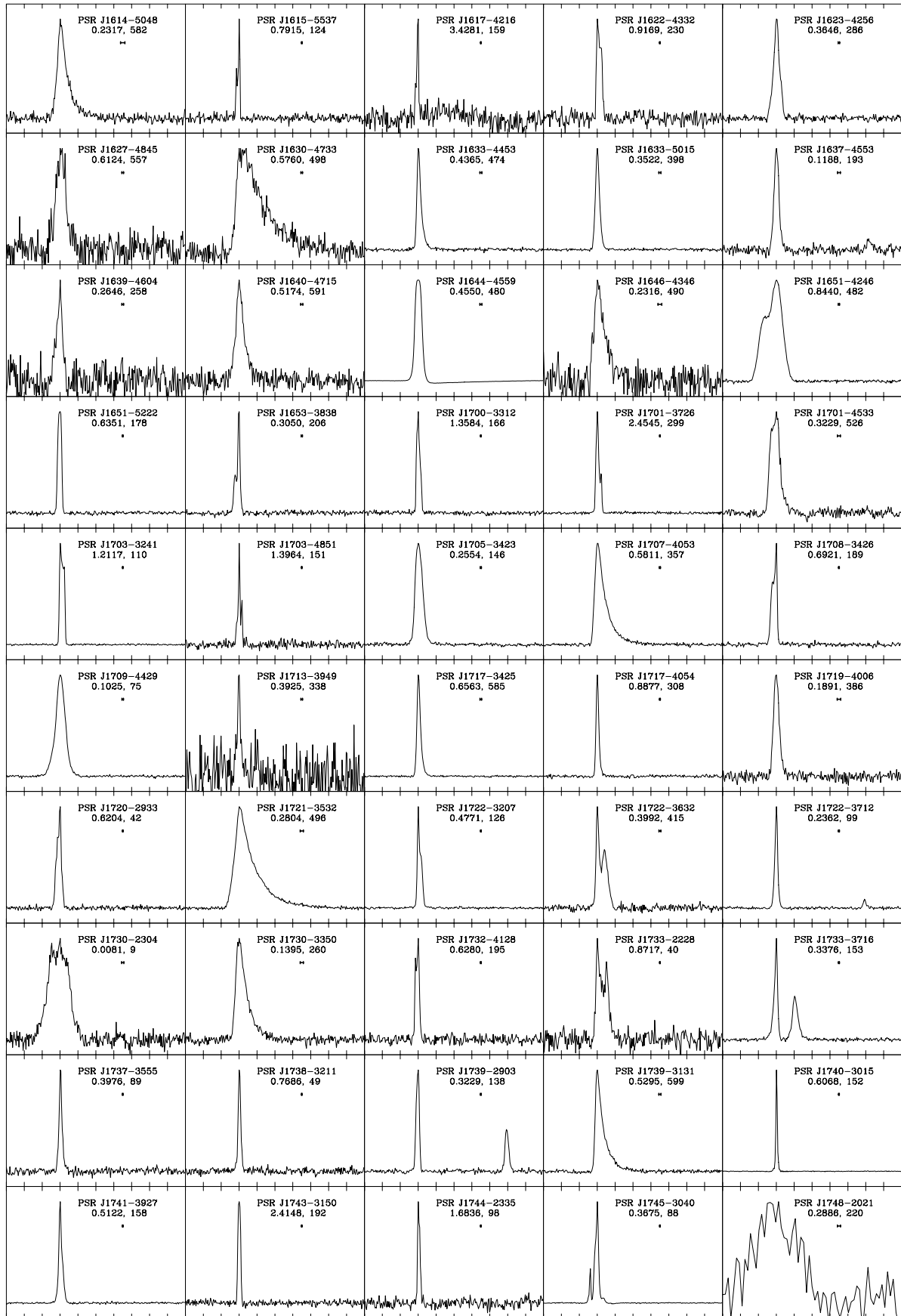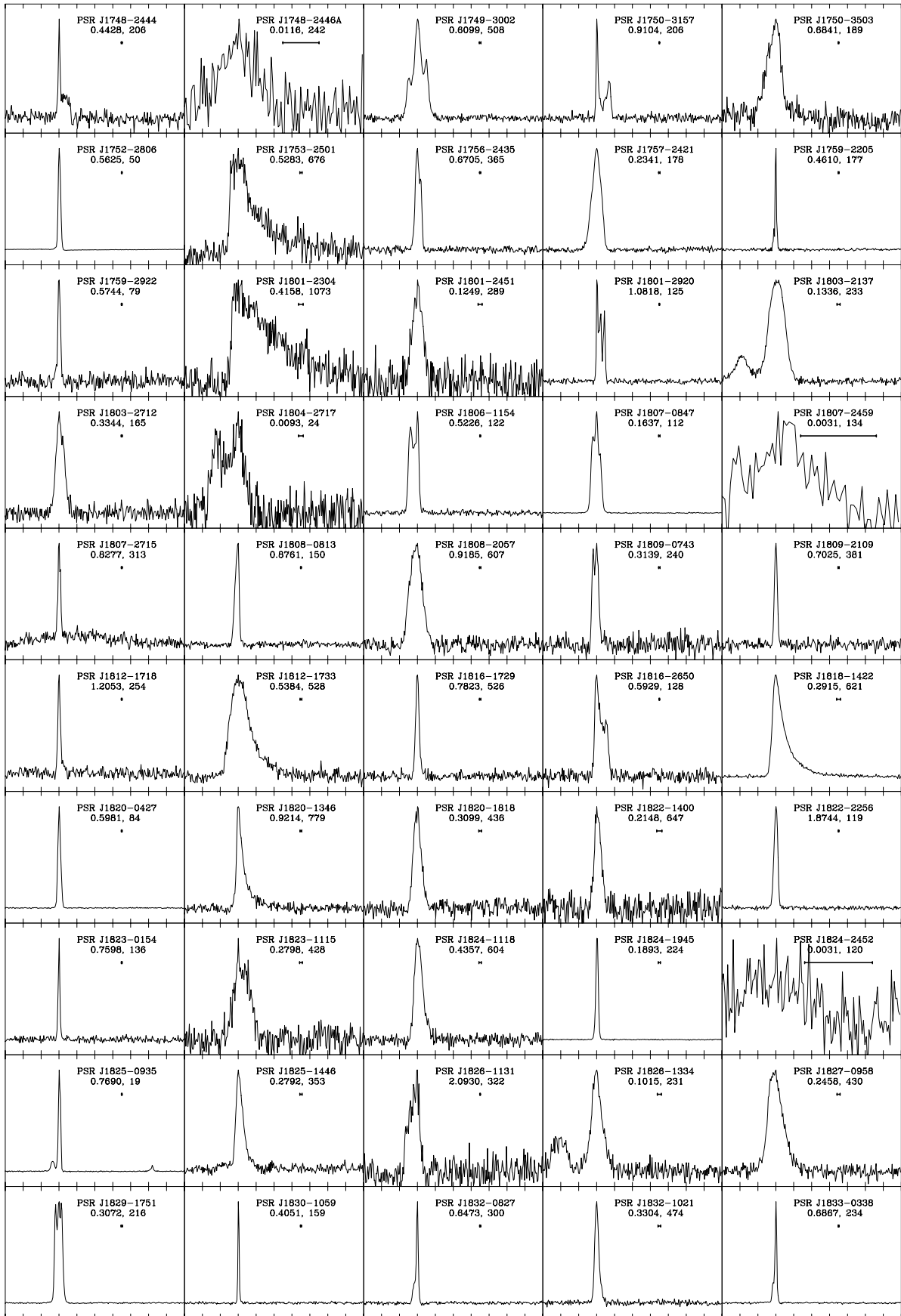
Figure 3 – *continued*

Figure 3 – *continued*

PSR J1748−2444
0.4428, 206

PSR J1748−2446A
0.0116, 242

PSR J1749−3002
0.6099, 508

PSR J1750−3157
0.9104, 206

PSR J1750−3503
0.6841, 189

PSR J1752−2806
0.5625, 50

PSR J1753−2501
0.5283, 676

PSR J1756−2435
0.6705, 365

PSR J1757−2421
0.2341, 178

PSR J1759−2205
0.4610, 177

PSR J1759−2922
0.5744, 79

PSR J1801−2304
0.4158, 1073

PSR J1801−2451
0.1249, 289

PSR J1801−2920
1.0818, 125

PSR J1803−2137
0.1336, 233

PSR J1803−2712
0.3344, 165

PSR J1804−2717
0.0093, 24

PSR J1806−1154
0.5226, 122

PSR J1807−0847
0.1637, 112

PSR J1807−2459
0.0031, 134

PSR J1807−2715
0.8277, 313

PSR J1808−0813
0.8761, 150

PSR J1808−2057
0.9185, 607

PSR J1809−0743
0.3139, 240

PSR J1809−2109
0.7025, 381

PSR J1812−1718
1.2053, 254

PSR J1812−1733
0.5384, 528

PSR J1816−1729
0.7823, 526

PSR J1816−2650
0.5929, 128

PSR J1818−1422
0.2915, 621

PSR J1820−0427
0.5981, 84

PSR J1820−1346
0.9214, 779

PSR J1820−1818
0.3099, 436

PSR J1822−1400
0.2148, 647

PSR J1822−2256
1.8744, 119

PSR J1823−0154
0.7598, 136

PSR J1823−1115
0.2798, 428

PSR J1824−1118
0.4357, 604

PSR J1824−1945
0.1893, 224

PSR J1824−2452
0.0031, 120

PSR J1825−0935
0.7690, 19

PSR J1825−1446
0.2792, 353

PSR J1826−1131
2.0930, 322

PSR J1826−1334
0.1015, 231

PSR J1827−0958
0.2458, 430

PSR J1829−1751
0.3072, 216

PSR J1830−1059
0.4051, 159

PSR J1832−0827
0.6473, 300

PSR J1832−1021
0.3304, 474

PSR J1833−0338
0.6867, 234

Figure 3 – *continued*

© 2004 RAS, MNRAS **352,** 1439–1472

Figure 3 – *continued*

Figure 3 – *continued*

3.2.2 Dispersion measures

For the pulsars listed in Table 9 we have obtained dispersion measure measurements more than an order of magnitude more precise than earlier results. Large discrepancies exist between the measured and previously determined dispersion measures for the three pulsars listed in Table 10. Small, but significant, changes in the absolute value of the dispersion measure may be accounted for by dispersion measure variations (see, for example, Hobbs et al. 2004). The largest discrepancy in Table 10 exists for PSR J0905−4536. Earlier archived observations of this pulsar from the Parkes telescope also suggest a much higher dispersion measure value than that obtained by D'Amico et al. (1998). We therefore believe that this earlier result was in error.

4 CONCLUSION

Observations for the Parkes multibeam pulsar survey have been completed. Processing of the data has so far led to over 700 new pulsar discoveries. Combining the new discoveries with redetections of previously known pulsars results in a sample of almost 1000 pulsars in the Galactic plane that have been analysed in a similar fashion. When we have completed processing the data from the multibeam survey, a well-defined sample of pulsars in the Galactic plane will exist with flux densities and dispersion measures all acquired in an identical manner. This sample will be used to update earlier studies of the pulsar population such as determining the pulsar birthrate and the total number of active pulsars in the Galaxy.

Table 8. Flux density measurements at 1400 MHz for those pulsars with no previously catalogued value at this observing frequency, but do have an earlier flux measurement at 400 MHz. If a value exists in the literature at 600 MHz then this is also provided along with the spectral index obtained from the 1400 and 400 MHz values. References for these flux density measurements are 1. Manchester, Newton & Cooke (private communication), 2. Qiao et al. (1995), 3. Manchester et al. (1996), 4. Lyne et al. (1998), 5. Stokes et al. (1986) 6. Lorimer et al. (1995) 7. Camilo & Nice (1995) 8. Lorimer, Camilo & Xilouris (2002), 9. Hulse & Taylor (1975) and 10. Costa, McCulloch & Hamilton (1991). Unfortunately, not all the S_{400} measurements have been published with corresponding uncertainties. Taking a typical uncertainty of 10 per cent leads to an error in the spectral index determination of ~ 0.3.

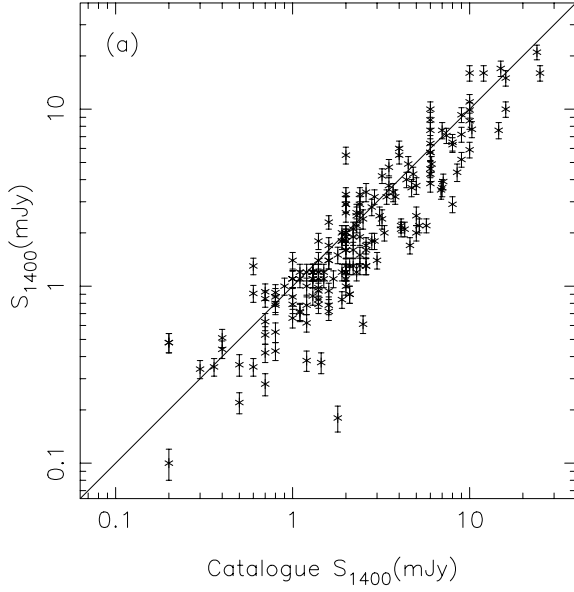| PSR J	PSR B	DM (cm^{-3} pc)	S_{1400} (mJy)	S_{400} (mJy)	S_{600} (mJy)	SI	Ref. S_{400}	Ref. S_{600}
J0828−3417	B0826−34	52.3(8)	0.25(4)	16	—	−3.3	1	—
J0842−4851	B0840−48	196.85(8)	0.62(7)	6.2	—	−1.8	1	—
J0904−4246	B0903−42	145.8(5)	0.60(7)	8	4	−2.1	1	2
J0905−4536	—	182.5(14)	0.83(9)	13	—	−2.2	3	—
J0924−5814	B0923−58	57.4(3)	4.3(4)	22	—	−1.3	1	—
J1042−5521	B1039−55	306.5(4)	0.62(7)	14	—	−2.5	1	—
J1112−6613	B1110−65	249.5(5)	2.6(3)	19	11	−1.6	1	10
J1121−5444	B1119−54	204.5(3)	1.30(14)	24	—	−2.3	1	—
J1123−6259	—	223.14(9)	0.56(7)	11	—	−2.4	4	—
J1239−6832	B1236−68	94.3(3)	0.96(11)	6.5	—	−1.5	1	—
J1259−6741	B1256−67	94.7(9)	1.30(14)	4.5	—	−1.0	1	—
J1326−6700	B1322−66	209.6(3)	11.0(11)	28	—	−0.8	1	—
J1603−5657	—	264.02(16)	0.53(6)	8	—	−2.2	4	—
J1622−4332	—	230.5(12)	0.53(6)	16	—	−2.7	4	—
J1700−3312	—	166.7(7)	1.20(13)	21	—	−2.3	3	—
J1703−4851	—	151.4(3)	1.10(12)	22	—	−2.4	3	—
J1705−3423	—	146.30(7)	4.1(4)	31	—	−1.6	3	—
J1732−4128	B1729−41	195.3(4)	0.63(7)	9	—	−2.1	1	—
J1806−1154	B1804−12	122.0(11)	2.6(3)	4	—	−0.3	5	—
J1816−2650	B1813−26	128.0(5)	1.10(12)	18	10.5	−2.2	6	6
J1834−0010	B1831−00	88.2(4)	0.29(4)	5.1	2.8	−2.3	6	6
J1848+0826	—	90.4(3)	0.11(2)	2.8	—	−2.6	7	—
J1854+1050	B1852+10	208(12)	1.03(14)	11	—	−1.9	5	—
J1901+0156	B1859+01	102.8(4)	0.38(5)	13.7	4.2	−2.9	6	6
J1902+0723	—	105.0(4)	0.17(3)	0.6	—	−1.0	7	—
J1904+1011	B1901+10	136.0(20)	0.58(7)	4.4	—	−1.6	8	—
J1908+0500	—	201.27(17)	0.79(9)	6.1	—	−1.6	7	—
J1908+0734	—	11.09(15)	0.54(6)	3.5	—	−1.5	7	—
J1908+0916	B1906+09	249.8(5)	0.23(3)	5	—	−2.5	9	—
J1910+0358	B1907+03	78.0(8)	1.50(16)	21	16	−2.1	6	6
J1910+0714	—	125.5(15)	0.36(5)	5.4	—	−2.2	7	—
J1910+1231	B1907+12	257.7(7)	0.28(4)	5	—	−2.3	9	—
J1912+1036	B1910+10	147.0(6)	0.22(3)	1.6	—	−1.6	8	—
J1913+0936	B1911+09	156.5(11)	0.14(2)	0.8	—	−1.4	8	—
J1914+1122	B1911+11	100(10)	0.55(7)	1.1	0.9	−0.6	6	6
J1915+0738	—	39.3(6)	0.34(4)	1.9	—	−1.4	7	—
J1930+1316	B1927+13	207.6(4)	0.18(3)	5	—	−2.6	9	—
J1933+1304	B1930+13	177.0(6)	0.42(5)	2.0	—	−1.2	8	—

© 2004 RAS, MNRAS **352**, 1439–1472

Figure 4. Flux density measurement comparisons. The new flux densities and previously published flux densities listed in Table 7 are compared. The solid lines indicate equality between the catalogued and measured flux values.

REFERENCES

Bailes M. et al., 1997, ApJ, 481, 386

Baring M. G., Harding A. K., 2001, ApJ, 547, 929

Blandford R., Teukolsky S. A., 1976, ApJ, 205, 580

Camilo F., Nice D. J., 1995, ApJ, 445, 756

Camilo F. et al., 2001a, ApJ, 557, L51

Camilo F. et al., 2001b, ApJ, 548, L187

Camilo F., Manchester R. N., Gaensler B. M., Lorimer D. R., 2002a, ApJ, 579, L25

Camilo F., Manchester R. N., Gaensler B. M., Lorimer D. L., Sarkissian J., 2002b, ApJ, 567, L71

Chen K., Ruderman M., 1993, ApJ, 408, 179

Clifton T. R., Lyne A. G., Jones A. W., McKenna J., Ashworth M., 1992, MNRAS, 254, 177

Cordes J. M., Lazio T. J. W., 2002, preprint (astro-ph/0207156)

Costa M. E., McCulloch P. M., Hamilton P. A., 1991, MNRAS, 252, 13

D'Amico N., Stappers B. W., Bailes M., Martin C. E., Bell J. F., Lyne A. G., Manchester R. N., 1998, MNRAS, 297, 28

Deich W. T. S., Middleditch J., Anderson S. B., Kulkarni S. R., Prince T. A., Wolszczan A., 1993, ApJ, 410, L95

Dowd A., Sisk W., Hagen J., 2000, in Kramer M., Wex N., Wielebinski R., eds, IAU Coll. 177, Pulsar Astronomy – 2000 and Beyond. Astron. Soc. Pac., San Francisco, p. 275

Edwards R. T., Bailes M., 2001, ApJ, 553, 801

Edwards R. T., Bailes M., van Straten W., Britton M. C., 2001, MNRAS, 326, 358

Gómez G. C., Benjamin R. A., Cox D. P., 2002, in Henney W. J., Franco J., Martos M., Peña M., eds, Rev. Mex. Astron. Astrof. Conf. Series, 12, 39

Haslam C. G. T., Stoffel H., Salter C. J., Wilson W. E., 1982, A&AS, 47, 1

Hobbs G., 2002, PhD thesis, Univ. Manchester

Hobbs G. et al., 2004, MNRAS, submitted

Hulse R. A., Taylor J. H., 1975, ApJ, 201, L55

Table 9. Dispersion measure values that have been measured more than an order-of-magnitude more precisely than in earlier studies. The earlier dispersion measures (DM$_{cat}$) and the new measurements (DM) have been obtained from Table 7.

PSR J	PSR B	DM$_{cat}$ (cm^{-3} pc)	DM (cm^{-3} pc)
J0842−4851	B0840−48	197.0(10)	196.85(8)
J0907−5157	B0905−51	104.0(7)	103.72(6)
J1001−5507	B0959−54	130(2)	130.32(17)
J1032−5911	B1030−58	419(5)	418.20(17)
J1107−5947	B1105−59	159(19)	158.4(11)
J1239−6832	B1236−68	96(5)	94.3(3)
J1326−6408	B1323−63	505(5)	502.7(4)
J1327−6222	B1323−62	318.4(9)	318.80(6)
J1340−6456	B1336−64	77(2)	76.99(13)
J1537−49	—	65(4)	65.0(3)
J1602−5100	B1558−50	172(1)	170.93(7)
J1639−4604	B1635−45	259(2)	258.91(4)
J1646−4346	B1643−43	490(5)	490.4(3)
J1717−3425	B1714−34	587.7(7)	585.21(6)
J1717−4054	B1713−40	317(9)	308.5(5)
J1732−4128	B1729−41	195(5)	195.3(4)
J1801−2451	B1757−24	289.0(10)	289.01(4)
J1826−1334	B1823−13	231.0(10)	231.09(8)
J1827−0958	B1824−10	430(4)	430.1(3)
J1833−0827	B1830−08	411(2)	410.925(12)
J1844+00	—	335(67)	345.54(20)
J1844−0310	—	836(7)	836.1(5)
J1845−0316	—	500(5)	500.00(14)
J1852+0031	B1849+00	787(17)	798.2(16)
J1859+00	—	412(82)	420(3)
J1901+00	—	346(69)	345.5(11)
J1905+0616	—	259(7)	257.9(6)
J1908+0916	B1906+09	250(20)	249.8(5)
J1916+07	—	305(30)	305.1(8)
J1916+1030	B1913+105	387(10)	387.2(3)

Table 10. DM measurements that are different from earlier work. Pulsars are included in this table if they are more than 3σ discrepant and have a difference in DM greater than 5cm^{-3} pc. References are 1. D'Amico et al. (1998) and 2. Newton, Manchester & Cooke (1981).

PSR J	PSR B	DM$_{cat}$ (cm^{-3} pc)	DM (cm^{-3} pc)	Ref.
J0905−4536	—	116.8(2)	182.5(14)	1
J1440−6344	B1436−63	124.2(5)	130.2(5)	2
J1651−4246	B1648−42	525(8)	482(3)	2

Johnston S., Lyne A. G., Manchester R. N., Kniffen D. A., D'Amico N., Lim J., Ashworth M., 1992, MNRAS, 255, 401

Kaspi V. M., Crawford F., Manchester R. N., Lyne A. G., Camilo F., D'Amico N., Gaensler B. M., 1998, ApJ, 503, L161

Kramer M., Xilouris K. M., Lorimer D. R., Doroshenko O., Jessner A., Wielebinski R., Wolszczan A., Camilo F., 1998, ApJ, 501, 270

Kramer M. et al., 2003, MNRAS, 342, 1299

Lommen A. N., 2002, in Becker W., Lesch H., Trumper J., eds, MPE Report 278, Neutron Stars, Pulsars, and Supernova Remnants. Max-Planck-Institut für extraterrestrische Physik, Garching, p. 114

Lorimer D. R., Xilouris K. M., 2000, ApJ, 545, 385

Lorimer D. R., Yates J. A., Lyne A. G., Gould D. M., 1995, MNRAS, 273, 411

Lorimer D. R., Camilo F., Xilouris K. M., 2002, ApJ, 123, 1750

Lyne A. G. et al., 1998, MNRAS, 295, 743

McLaughlin M. A. et al., 2003a, ApJ, 591, L135

McLaughlin M. A. et al., 2003b, in Camilo F., Gaensler B. M., eds, ASP Conf. Proc., IAU Symposium 218, Young neutron stars and their environment. Astron. Soc. Pac., San Francisco, in press

Manchester R. N., Lyne A. G., Taylor J. H., Durdin J. M., Large M. I., Little A. G., 1978, MNRAS, 185, 409

Manchester R. N. et al., 1996, MNRAS, 279, 1235

Manchester R. N. et al., 2001, MNRAS, 328, 17

Maron O., Kijak J., Kramer M., Wielebinski R., 2000, in Kramer M., Wex N., Wielebinski R., eds, IAU Coll. 177, Pulsar Astronomy – 2000 and Beyond. Astron. Soc. Pac., San Francisco, p. 227

Mohanty D. K., 1983, in Danziger J., Gorenstein P., eds, IAU Symp. 101, Supernova Remnants and their X-ray emission. Dordrecht, Reidel, p. 503

Morris D. J. et al., 2002, MNRAS, 335, 275

Newton L. M., Manchester R. N., Cooke D. J., 1981, MNRAS, 194, 841

Nice D. J., Fruchter A. S., Taylor J. H., 1995, ApJ, 449, 156

Qiao G. J., Manchester R. N., Lyne A. G., Gould D. M., 1995, MNRAS, 274, 572

Reich P., Reich W., 1988, A&A, 196, 211

Stokes G. H., Segelstein D. J., Taylor J. H., Dewey R. J., 1986, ApJ, 311, 694

Tauris T. M., van den Heuvel E. P. J., 2003, preprint (astro-ph/0303456)

Tauris T. M., van den Heuvel E. P. J., Savonije G. J., 2000, ApJ, 530, L93

Taylor J. H., Cordes J. M., 1993, ApJ, 411, 674

Toscano M., Bailes M., Manchester R., Sandhu J., 1998, ApJ, 506, 863

Van Vleck J. H., Middleton D., 1966, Proc. IEEE, 54, 2

This paper has been typeset from a TEX/LATEX file prepared by the author.